# MULTIPLE WILDFIRE DISTURBANCES AMPLIFY SEASONAL MOISTURE STRESS IN A MOIST, MIXED-CONIFER MONTANE ECOSYSTEM

By

GREGORY DANIEL CLARK

A thesis submitted in partial fulfillment of
the requirements for the degree of

MASTER OF SCIENCE IN ENVIRONMENTAL SCIENCE

WASHINGTON STATE UNIVERSITY
School of the Environment

JULY 2018

To the Faculty of Washington State University:

The members of the Committee appointed to examine the thesis of GREGORY DANIEL CLARK find it satisfactory and recommend that it be accepted.

Kevan B. Moffett, Ph.D., Chair

Andrés Holz, Ph.D.

Markus Flury, Ph.D.

Marc G. Kramer, Ph.D.

# ACKNOWLEDGMENT

First and foremost, I wish to thank my advisor, Dr. Kevan Moffett, founder of the Hydrology, Ecohydrology, and Landscape Dynamics research group, for her continuous support for the Mount Adams project. She has been a continuous source of encouragement and mental sanity throughout the duration of my work. Kevan has supported me through her wealth of research expertise and organizational skills while completing my own research and writing. Thanks to her, I had the opportunity to work in a beautiful location studying what I love.

I want to thank my thesis committee, Andres Holz, Markus Flury, and Marc Kramer, for their guidance and constructive comments while writing my thesis. Each of the members possessed valuable expertise that they shared to help me learn and navigate scientific research.

Thanks to the Geological Society of America, whose graduate student research grant helped make this project possible.

I am beyond grateful to all those who have helped me in the field collecting data for this project I am especially grateful to the members of the members of the Hydrology, Ecohydrology, and Landscape Dynamics research group, Allan Jones, Katherine Swensen, Sarah Kintner, Matthew Pruett, Gerald Page, and Peter Zemora for their continuous voluntary support during the field season. Those who have also helped serve as important additions to the field crew include: Ethan Bean, Sebastian Busby, Samantha Bussan, and Niall Millar. Thank you.

Finally, I would like to thank my parents, whose encouragement and emotional support helped me survive the long northwest winters.

MULTIPLE WILDFIRE DISTURBANCES AMPLIFY SEASONAL MOISTURE STRESS IN A MOIST, MIXED-CONIFER MONTANE ECOSYSTEM

Abstract

by Gregory Daniel Clark, M.S.
Washington State University
July 2018

Chair: Kevan B. Moffett

Wildfire is an important ecosystem function in many forested landscapes, promoting resilience and biodiversity, but it also causes significant disturbances to forest soils and hydrology. Alterations to soil structure and fire-induced hydrophobicity can often lead to significant water-stress during summer drought in seasonally dry environments. To asses near surface soil moisture dynamics and its relation to surface cover over the course of the dry season on hillslopes recovering from recent fire we compared soil moisture measurements across a gradient of burn histories. We monitored soil moisture at 15 and 50cm and conducted periodic electromagnetic induction surveys in four areas with different burn histories aimed at sensing moisture differences. Soil moisture drydown was rapid, reaching permanent wilting point 2-3 weeks after snow disappearance. The rate of soil drying was relatively indistinguishable between burned plots of varying burn histories, but all burned plots dried significantly faster than an unburned patch of forest. With the return of precipitation in October, apparent conductivity in the burned soils remained relatively constant, with the exception of the plot affected by recurrent fire whose apparent conductivity decreased. These observations suggest a persistence of fire induced hydrophobicity. Soil moisture was correlated with surface cover, with the highest moisture contents occurring beneath dense plant cover and coarse woody debris.

## TABLE OF CONTENTS

## LIST OF TABLES

## LIST OF FIGURES

## Dedication

This thesis is dedicated to my grandfather, whose passion for the natural world inspired my own.

## 1. Introduction

Wildfire is an important ecosystem function in many forested landscapes, promoting resilience and biodiversity. Prior to twentieth century fire suppression strategies, wildfires occur every 200-500 years in western Pacific Northwest forests (Agee, 1996). However, as wildfire return intervals are shortening, forest recovery suffers (Collins et al., 2009). Many forested ecosystems in the western United States are expected to continue experiencing increasingly warm, dry climates resulting in forests more susceptible to pests, disease, and wildfire (Dennison et al., 2014; Bladon et al., 2014). The loss of western forests due to fire presents watershed and forest managers with numerous issues including increased erosion, debris flows, elevated runoff temperatures (Debano et al., 1998), higher risk of drought and low river flows (Bixby et al., 2015), and export of harmful compounds produced by fire (Vehniäinen et al., 2016). Understanding that forest recovery is an important process in mitigating harmful effects of fire on watershed hydrology, researchers have extensively examined ecosystem recovery and alterations to hillslope hydrology. Many studies have focused on changes to water quantity and quality at the catchment scale in fire-affected ecosystems, finding increases to runoff discharge (Moody and Martin, 2001; Mayor et al., 2007) and sediment loads carrying excess nutrients and heavy metals (Smith et al., 2011; Murphy et al., 2006). Few consider alterations to water quantity and availability held in post-fire soils (Melgoza et al. 1990; Boisramé et al., 2018).

It is well documented that fire can have a profound effect on soil physical properties depending on the fire duration, intensity, and moisture content of the soil (Shakesby, 2011; Cerda, 2009; Cerda and Robichaud, 2009). For example, soil heating results in reductions of soil organic matter (Alauzis et al., 2004; Mora et al., 2015), decreased aggregate stability (Certini, 2005;

Andreu et al., 2001), and consequently decreased porosity and increased bulk density (Andreu et al., 2001; Stoof et al., 2010). Combustion of the thin layer of decomposed organic material that lies between the A horizon and litter layer, also known as duff, and incomplete combustion of incorporated soil organic matter, can result in fire-induced hydrophobicity (Doerr et al., 2000). Fire-induced hydrophobicity then decreases soil water retention (Ebel, 2012) and infiltration capacity (Stoof et al., 2010).

Reduced infiltration rates caused by hydrophobicity and soil compaction not only suggest increased runoff and erosion but may also imply reduced moisture retention and limited soil moisture availability throughout the growing season. While forest recovery is often dependent on nutrient availability (DeBano et al., 1998; Neary et al., 1999), soil moisture is also an important controlling factor in seasonally dry environments and is often overlooked (Abbot and Roundy, 2003; Duniway et al., 2015). With projections of longer fire seasons and increased wildfire occurrences resulting from climate change (Westerling et al., 2006), there is a need to investigate how forests and their underlying soils are responding to fire disturbances and the possible consequences of recurrent wildfire, i.e. consecutive fires occurring on the same land surface less than 20 years apart. Recurring wildfire leads to extensive exposure of bare soil surface through depletion of vegetative cover and a more complete consumption of the duff layer; this exposure of the soil surface after multiple wildfires consequently increases the risk of soil erosion and degradation (Loaiciga et al., 2001; Wittenberg and Inbar, 2009; Malkisnon, 2011; Hosseini et al., 2016). Repeated burns resulting in more complete combustion of coarse woody debris may also have direct effects on post-fire soil heating and moisture retention. Researchers have started investigating this gap in knowledge by studying forest patches subjected to artificially induced

recurrent fire (Hatten et al., 2012; Lombao et al., 2015), with no studies directly exploring moisture availability on hillslopes affected by naturally occurring short-interval wildfires. Given current trends in changing climate, hydrology, and ecosystems, alterations to soil water retention in fire affected landscapes may be of increasing concern to watershed and forest managers, particularly if recurring fires are significantly prolonging drought stress. The combination of increasing wildfire activity and post-fire drought stress may lead to dramatic biogeographical shifts in forested ecosystems, such as changes in the extent of dry shrublands and other drought tolerant ecotones (Harvey et al. 2016).

Given the importance of the topic and the currently sparse data on *in situ* forest soil moisture during post-wildfire ecosystem recovery, the aims of this study were to investigate how wildfires influence moisture availability during the summer dry season and its relation to vegetative reestablishment. Specifically, we asked: (1) How does fire influence plant available water and the duration of its availability following snow disappearance? We expected burned soils to have more plant available water and longer growing seasons due to reduced interception and transpiration. (2) What role does water serve as a resource for plant recruitment in post-fire environments affected by seasonal drought? We expected post-fire vegetation to be concentrated in areas of higher water content, particularly deeper rooting tree saplings and shrubs. (3) What are the possible consequences of short-interval recurrent wildfire with respect to soil properties and soil moisture? We expected short-interval wildfires to have a significantly compounded influence on soil properties, particularly bulk density and organic matter. We also expected soils affected by recurrent fire to have an accelerated period of soil moisture drying.

## 2. Methods

To assess impacts of post-fire regrowth intervals on soil moisture availability and rates of depletion through the summer, we monitored a gradient of varying burn histories using a combination of continuous soil moisture and temperature measurements at shallow depths as well as monthly geophysical measurements from July to October 2017, capturing the duration of the dry season after snowmelt.

### 2.1 Site Description and Experimental Set-up

The field site was located on the southern slope of Mount Adams in the Gifford Pinchot National Forest in southern Washington State (Figure 1A). The site is on a moderately steep hillslope approximately 1400m above mean sea level at the intersection of the Cascade Crest Montane and Grand Fir Mixed Forest ecoregions (Omernik, 1987). The site overlays middle Miocene Grande Ronde Basalt (Korosec, 1987). Tree species within the Cascade Crest Montane and Grand Fir Mixed Forest ecoregions largely consist of *Tsuga mertemsiana, Abies amabilis, Picea englemannii, Pinus ponderosa*, *Psuedotsuga menziessii,* and several species of grass and forb (Franklin and Dyrness, 1988). To the best of our knowledge, the average wildfire return intervals for this forest type and ecosystem range between 73 and 246 years (Olson and Agee, 2005), with shorter intervals in drier areas and longer intervals in wetter areas. The climate of the site is strongly seasonal, with predominantly winter precipitation, snow cover persisting 5-7 months of the year, and very little summer precipitation. This climate regime and ecoregion presents and ideal opportunity to study water limitation in a recovering montane forest, in any given year. Being located on the southern slope of the mountain, the site is neither on the very wet windward side of the Cascade Range, nor in the dry rainshadow of the eastern side; it resides among

intermediate montane climate conditions. The 30-year average annual precipitation is 2085 mm. Total precipitation for the 2016 water year was 2332 mm, which increased in 2017 to 2581 mm (PRISM Climate Group, 2018). The maximum snow water equivalent measured at the nearest climate station (25 km west of the study site and about 100 m lower in elevation) was 166cm during water year 2017 was well above the 30-year median of 115cm (NRCS Snotel- 804). The site lies within the White Salmon River watershed.

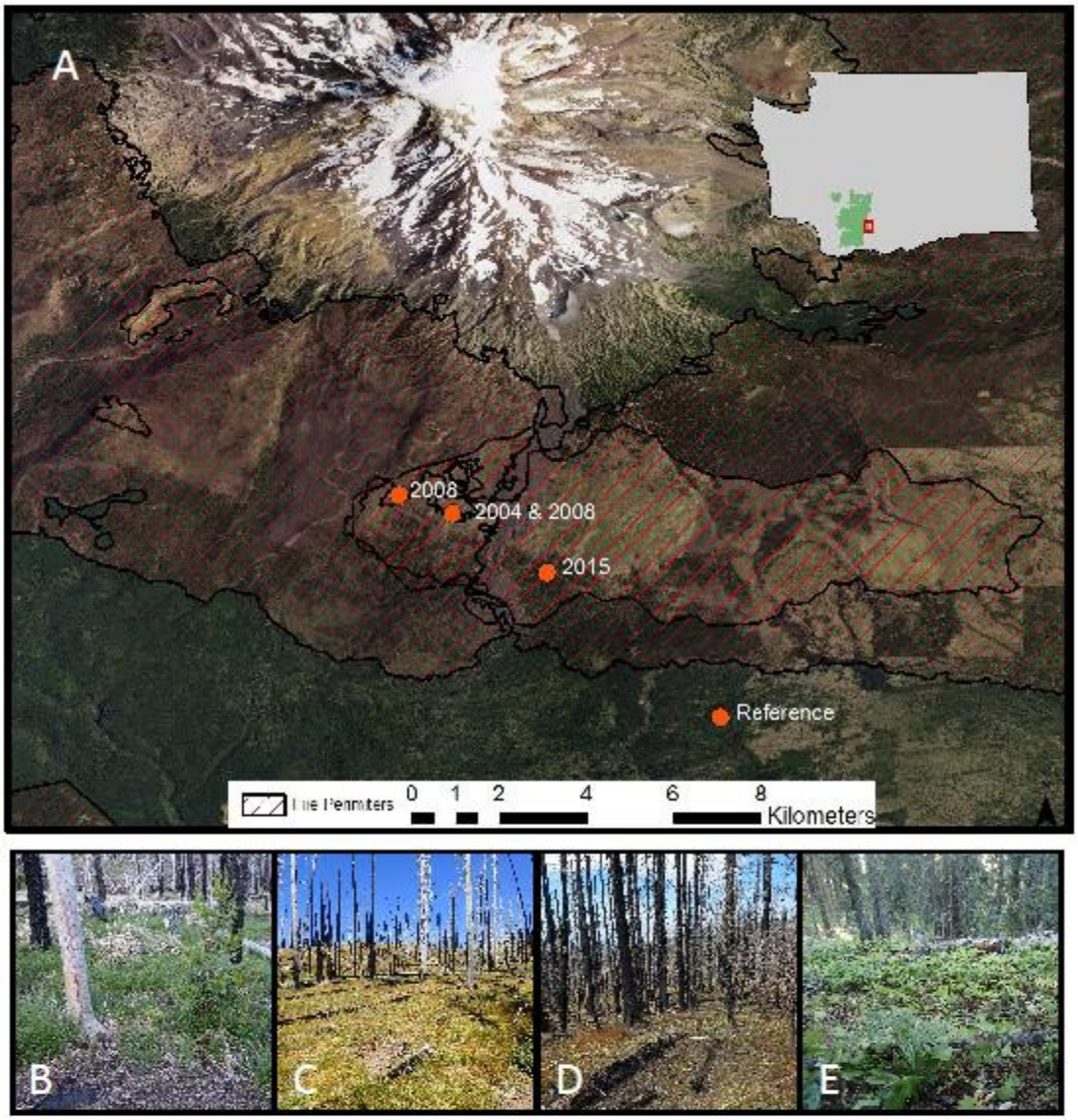


Figure 1. (A) Overview of the southern slope of Mount Adams, Washington, locations of past wildfires, and field plots. Burn scars are marked by red hashing and black outlines, and the research plot locations are marked with orange dots. Inset: Study region location (red box) in Washington State (grey, WDNR) and the Gifford Pinchot National Forest (green, USDA-FS). Research plots experienced different burn histories, as visible in site photos: (B) burned only in 2008, (C) both in 2004 and 2008, (D) and only in 2015. Understory vegetation in the unburned reference (E) is markedly different than the burned plots (B, C, D).

We selected four research plots of similar gradient, aspect, elevation, geologic parent material, climate, ecosystem, and land use history, but each having a unique burn history in terms of

number of burns and time of recovery since the most recent wildfire (Table 1). One site was affected by the 2008 Cold Springs fire (Figure 1B), another was affected the 2008 Cold Springs fire and the 2004 McDonald Ridge fire (Figure 1C), and the third burned hillslope was affected only by the 2015 Cougar Creek fire (Figure 1D). For simplification, we named the burned hillslopes B-08, B-04/08, and B-15. The twice-burned hillslope was established to investigate the possible influence of recurrent fire on soil hydrologic properties. On each burned hillslope, we established 0.25 ha study plots. A smaller 0.05 ha plot was established at the reference site due to limited space at the nearest location external to all burn perimeters but with comparable slope, aspect, and elevation as the burned plots (Figure 1E). We called this hillslope UB. The averages and standard deviations of the elevations, slopes, and aspects of the four research plots were 1375±68 m above mean sea level, 9.19±1.48 degrees, and 229.25±11.53 degrees from North (Table 1). To address the focus on dry-season moisture availability for recovering post-fire forest ecosystems, field measurements were conducted during the summer, primarily in 2017 and during baseflow conditions. Local hydrological conditions in the study year are summarized in Figure 2.

Table 1. Summary of study plot topographical characteristics

| Plot | Unburned UB | Burned B-08 | Burned B-04/08 | Burned B-15 |
|---|---|---|---|---|
| Latitude | 46.076 | 46.122 | 46.118 | 46.106 |
| Longitude | -121.438 | -121.504 | -121.493 | -121.474 |
| Elevation (m) | 1327 | 1418 | 1447 | 1308 |
| Slope (Deg.) | 9.48 | 9.48 | 7.13 | 10.65 |
| Aspect (Deg.) | 231 | 230 | 214 | 242 |

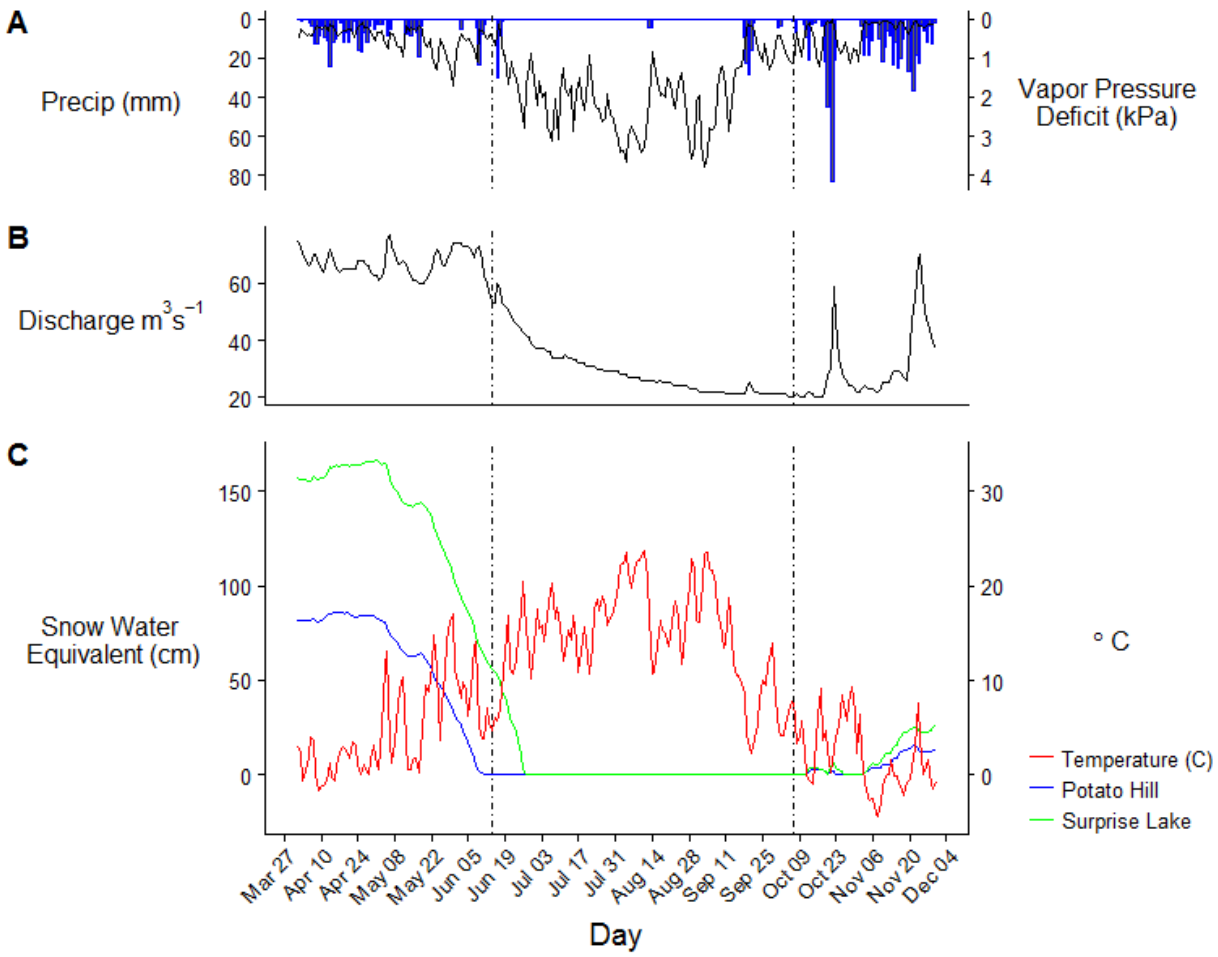


Figure 2. Regional hydrologic conditions for April-December 2017. The study spanned the duration of the dry season from late June to September (between vertical dashed lines), when little to no precipitation occurred after snow disappearance (A). Snow water equivalent at the site is expected to fall between the data from the two nearest SNOTEL sites (C, blue, green lines, left axis). The summer dry season is also the warmest part of the year for this region (C, red line, right axis) and exhibits baseflow conditions in the White Salmon River (B). (A) from PRISM Climate Model. (C)Snow water equivalent from NRCS SNOTEL stations Potato Hill (Station #702; 46.35, -121.51) and Surprise Lakes (Station #804; 46.09, -121.76). (C) Average temperature from PRISM Climate Model. (B) from USGS gage 14123500 (45.75, -121.53).

## 2.2 Continuous Soil Moisture Monitoring

To analyze temporal changes in soil moisture on each hillslope, we installed soil moisture sensors at two depths, 15cm and 50cm, in all plots. Four probes were placed at each depth for a

total of eight sensors per plot. All 15cm soil moisture sensors were Hydraprobe dielectric soil water probes (Stevens Water Monitoring Systems, Portland, OR). All 50 cm soil moisture sensors were Decagon-5TM probes (Decagon Devices, Pullman, WA). All soil moisture and temperature probes utilized a loam calibration and were evenly spaced at 10m from the centrally located Campbell CR300 datalogger to which they were attached. Probes were placed under patches of bare soil and grass to avoid disturbing living shrubs and coarse woody debris. Sensors were set to record soil moisture and temperature every 30 minutes. We then computed daily averages for each study plot and each depth.

### 2.3 Spatial Measurements of Soil Moisture

To obtain a more spatially exhaustive interpretation of soil moisture across each research plot, we conducted periodic geophysical measurements. We conducted electromagnetic induction (EMI) surveys at the beginning of each month from July through October throughout all four plots. EMI surveys measured near surface apparent conductivity (ECa) at two depths of integration: 0.3m and 0.5m. We used ECa as a proxy measurement for soil water content due to the low magnitude and narrow range of salinity and clay contents in the soil.

EMI has been utilized heavily in precision agriculture for estimating soil and water properties such as salinity, clay content, and soil depth (Lesch et al., 2005; Zhu et el., 2010; Doolittle and Brevik, 2014; Serrano et al., 2013). Recently, EMI methods have begun to be used in studies of natural systems for measuring subsurface properties ranging from salinity to estimating bulk soil physical properties (Robinson et al., 2008; Moffett et al., 2010; Abdu et al., 2008; Franz et al., 2011; Sherlock and McDonnell, 2003). EMI is a useful method for measuring soil properties due

to its non-invasive nature and capability for rapid, spatially exhaustive data collection (Corwin and Lesch, 2003). Measured ECa represents the soil electrical conductivity integrated over the depth of exploration (DOE) (Callegary et al., 2007; Hendrickx et al., 2002). Measured ECa is most notably influenced by soil clay content, volumetric water content, and salinity within the DOE (Rhoades et al., 1976; Friedman, 2005). For this study, we collected ECa data using a Dualem-1H instrument (Dualem, Milton, ON). The instrument has both horizontal coplanar (HCP) and perpendicular (PRP) configurations, each with two array lengths. For this study, we used the PRP configuration due to its shallow DOE. The 0.6m and 1.1m PRP array lengths had approximate DOEs of 30cm and 50cm, yielding raw ECa data for the 0-30cm and 0-50cm soil depth intervals when the EMI instrument was set on the soil surface for measurements.

In each of the 0.25ha burned plots, each monthly EMI survey consisted of thirteen, evenly-spaced, 48m-long transects oriented perpendicular to the slope. Transects were spaced 4 m apart and ECa was recorded every 4m to produce 169 gridded point measurements per plot. In the 0.05ha unburned reference plot, each EMI survey consisted of four 48m-long transects, perpendicular to the slope, and measurements recorded every 4m along each transect to generate a 52-point grid. For each measurement, the EMI instrument was placed on the soil surface to achieve the maximum DOE and limit resistive air space between the instrument and the soil. When obstacles (e.g., coarse woody debris or standing dead trees) prevented precise location sampling, measurements were recorded as close as possible to the intended location while noting the distance from the desired location. Quality assurance/control procedures were applied to each survey to remove any significant outliers. This was accomplished by producing histograms of each survey to determine the range of apparent conductivity producing a smooth frequency

distribution of points. We then plotted ECa as a time-series and removed unexpected outliers. We also used variogram analysis to assess spatial autocorrelation and distribution of ECa.

The effective range of ECa for all plots was 0-30 mS $m^{-1}$. Negative values were interpreted as significantly low ECa values and corrected to a minimum ECa of 0 mS $m^{-1}$. Remaining values were then temperature-corrected to 25°C using initial temperatures measured by the installed soil moisture probes and standard conversion functions proposed by Sheets and Hendricks, 1995. ECa data collected from the 30cm and 50cm DOEs were then converted to layer-specific bulk soil electrical conductivity values ($\sigma$) for soil layers of depths 0-30cm and 30-50cm. No adjustment was needed for the shallower (0-30cm) soil layer, as the shallow ECa data were used directly as ECa(DOE=30cm) = $\sigma_1$. To determine the bulk soil electrical conductivity for the deeper 30-50cm layer, we rearranged the equation described by McNeill and Bosnar (1999)

$$ECa = \sigma_1 [1 - C_1] + \sigma_2 [C_1 - C_2] \quad (1)$$

to solve for $\sigma_2$:

$$\sigma_2 = (ECa - \sigma_1 [1 - C_1]) / [C_1 - C_2] \quad (2)$$

In equations (1) and (2), ECa is the value measured by the EMI over the deeper DOE 0-0.5m, which is a depth-weighted average of the electrical conductivities of discrete soil layers, $\sigma_1$ and $\sigma_2$. $C_1$ and $C_2$ are the cumulative EMI responses to the bottom of each respective layer. The Cumulative response function was taken from McNeill, 1980. All EMI results presented in this paper are presented as layer-specific soil electrical conductivity values. For simplicity we refer to

$\sigma_1$ for soil layer 0-30cm as $ECa_1$ and $\sigma_2$ for soil layer 30-50cm as $ECa_2$, throughout, and use ECa units mS $m^{-1}$.

## 2.4 Soil Properties and Water Retention

To assess similarities and differences in soil properties among plots and aid interpretation of the EMI data, we collected 12 soil cores from each research plot using a response surface sampling design developed with the ESAP software package (Lesch, 2006). Response surface-guided sampling allowed us to confidently sample from the full range of ECa for each plot while identifying objective and pseudo-random field locations to core in advance (Lesch et al., 2000; Lesch, 2005; Brus and Heuvelink, 2007). A preliminary EMI survey of each plot from October 2016 was used in the response surface analysis to design the soil collection plans. At each of the twelve sampling locations per plot, cores were collected of the top 30cm using a T-bar probe (AMS; inner diameter 2cm) in July 2017. Volumetric water content and soil bulk density were determined from sample mass measurements before and after standard oven drying at 105 °C, assuming a particle density of 2.65 g/$cm^3$ and water density of 1.00 g/$cm^3$. After drying, and after removing large stones from the soil using a #10 sieve, we estimated sand, silt, and clay mass fractions using the sedimentation-hydrometer method (Gee and Or, 2002), measured electrical conductivity of saturated paste extract (ECe; Robbins and Wiegand, 1990), and quantified soil organic matter (SOM) from mass loss on ignition (Schulte and Hopkins, 1996). Potential differences in bulk soil properties among the four field plots were statistically analyzed in R using ANOVA.

Saturated hydraulic conductivity was determined using a Minidisc Infiltrometer and supplied macros (Meter Group, Pullman, Washington). Infiltrometers were placed at each soil sampling location (N = 15) using a pressure head of -2 cm. In addition to saturated hydraulic conductivity, water retention curves were determined for soils from each field plot, using the evaporation method and a HYPROP instrument (UMS, Munich, Germany). Bulk soil samples from the top 15cm were collected from each of the soil moisture probe locations using a hand trowel and homogenized for each study plot. Subsamples were repacked into the Hyprop rings to the average bulk densities of the previously measured cores from the corresponding study plot. The Hyprop samples were then saturated in a bath of deionized water for 24h. Two tensiometers were installed at depths of 12.5mm and 37.5mm below the sample surface, which recorded changes in matric potential as the sample dried evaporatively (Schindler et al., 2010). Samples were weighed throughout the drying period to measure changes in mass. The van Genuchten functions for soil water retention (Van Genuchten, 1980) were fit to the measured retention curves to derive hydraulic parameters using the Hyprop analysis software (Hyprop-Fit, Meter Group, Munich, Germany).

## 2.5 Surface Cover Abundance

An initial, detailed vegetation survey of each plot was conducted in August 2016. Three transects, spaced 12m apart and parallel to slope, were established in the center of each plot. Each transect consisted of 10 sampling points spaced every 4 m for a total of 30 sampling points per research plot. At each sampling point, a 1m quadrat was placed and each species occurring within the quadrat was recorded. A table of all vegetation species detected is provided in the Supplement. The ten most abundant plant species observed were: *Carex rossii, Xerophyllum*

*tenax, Penstemon euglaucus, Achnatherum occidentale, Prunus emarginata, Adenocaulon bicolor, Achyls triphylla, Lupinus lepidus, Bromus inermis, Agastache occidentalis.*

Since such detailed species-level sampling would have been prohibitive to do in a spatially-exhaustive manner throughout the large field plots, for spatially-distributed cover mapping we conducted categorical surface cover functional type characterization using the Braun-Blanquet relative abundance method (Braun-Blanquet, 1932). For a 2x2m quadrat centered over each EMI survey point (n=169 per burned plot, n=52 in reference plot), observable surface cover was categorized into six classification bins: living tree, shrub, forb/herb, graminoid, coarse woody debris, or bare soil surface (Tinker and Knight, 2000; Pierson et al., 2001; Wilcox et al., 1988). We defined coarse woody debris as fallen tree limbs and trunks greater than 8cm in diameter. We assigned each 2x2m sampling frame a Braun-Blanquet scale value for each of the six cover categories using the scale presented in table 2.

Table 2. Braun-Blanquet scale classifications in relation to percent cover.

| Braun-Blanquet Scale | Range of Abundance (%) |
|---|---|
| 5 | 75 -- 100 |
| 4 | 50 -- 75 |
| 3 | 25 -- 50 |
| 2 | 5 -- 25 |
| 1 | <5 |
| + | trace |
| 0 | absent |

These categorical rankings of surface cover were then compared with each other in relation to measured ECa and the relative abundance of each sampling location.

## 3. Results

### 3.1 Soil Properties

Figure 3. Typical soil profile found at all burned research plots with an A-horizon >50cm in depth.

Lack of USDA Soil Survey data coverage for the study area made it difficult to determine the soil series. From nearby soil survey coverage and observations made in the field, we determined all study plot soils are of the Waaw series. Waaw soils are characterized as deep, well drained soils formed on mountain sideslopes. Their taxonomic class is mixed Humic Xeric Vitricryands.

The soils in all plots were coarse-textured in the top 30cm. There was no apparent change in soil horizon extending down to 50cm (Figure 3). Average clay content ranged from 8.57% in UB to 5.12% in B-04/08 (Figure 4, Table 3). Sand content ranged from 75% to 79%. Average organic matter (OM) fraction was higher in UB, at 15.33%, compared to the burned sites, which had average OM ranging from 8.2-9.3%. Soils were found to be non-saline with a range of 0-3 mS $m^{-1}$ soil electrical conductivity as determined with Hydraprobes. This was confirmed in the laboratory using saturation paste extract (ECe) from October 2016 samples which also ranged from 0-3 mS $m^{-1}$.

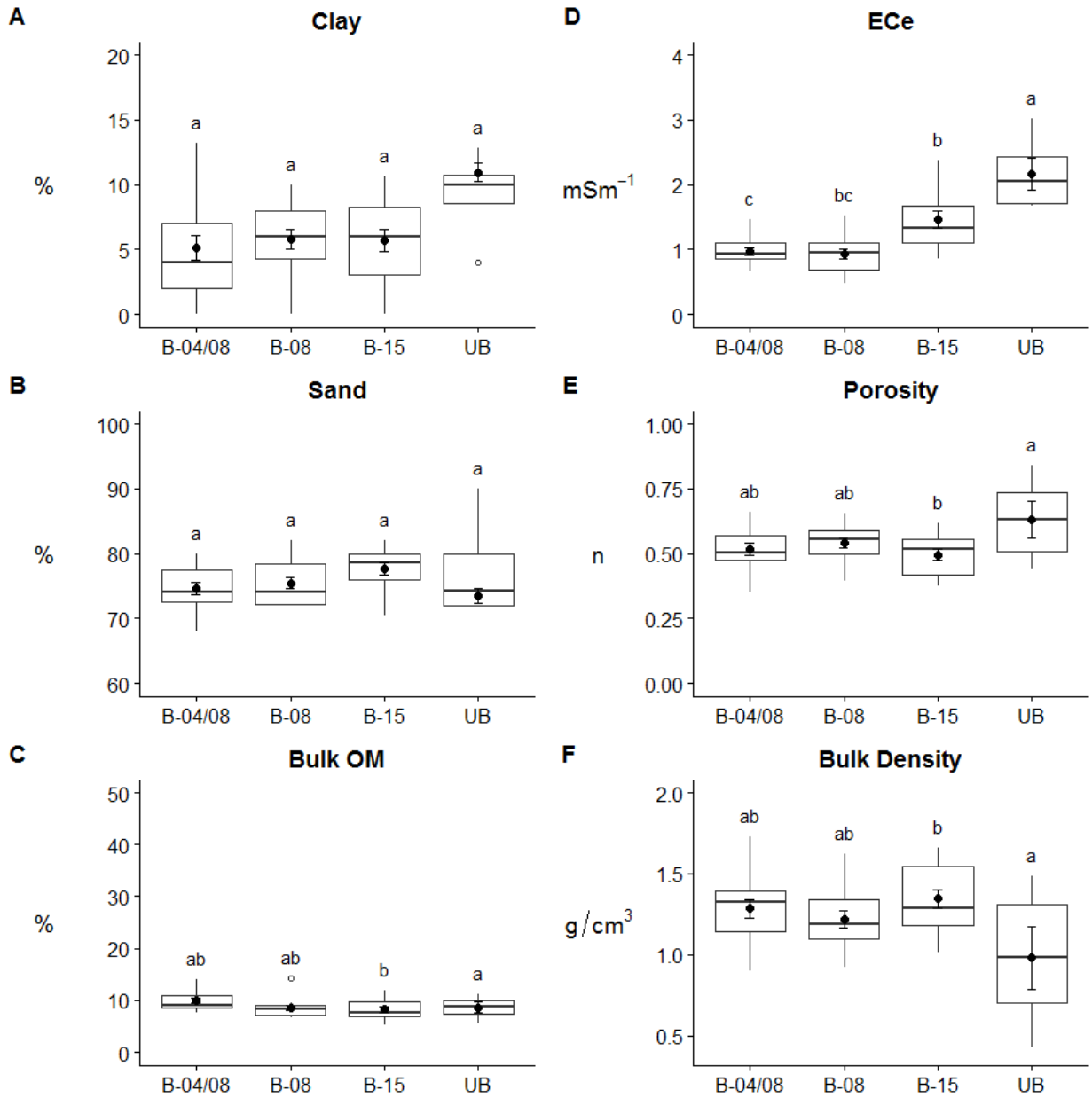


Figure 4. Summary of soil properties per field plot. (A-F) are boxplots of soil physical properties with the solid line representing the median (N=12). The box ends represent the 25$^{th}$ and 75$^{th}$ percentile, while the whiskers represent the 10$^{th}$ and 90$^{th}$ percentiles. Outliers are shown as open points. The solid point is the mean ± S.E. Letters indicate Tukey's pairwise groupings where shared letters are not significantly different. (A-B) are particle size fractions by weight. (C) is the mass fraction of bulk organic matter expressed as a percent. (D) is soil saturation paste extract electrical conductivity in mSm$^{-1}$. (E) is porosity as a volume fraction. (F) is dry bulk density of the top 30cm of each plot.

There was no significant difference in soil texture (sand, silt, or clay fractions) among plots (Table 3). As expected due to its undisturbed soil aggregates, UB had the highest porosity with a mean of 49.5%; this was significantly different from B-15 ($p= 0.037$). A spearman's rank correlation indicated porosity was weakly correlated with time since the most recent burn (Spearman's $\rho= 0.258$, $p= 0.076$), with the lowest soil porosity occurring in B-15. There was a small, significant difference in soil ECe among research plots ($p= 4.07e-06$). A Tukey's pairwise comparison indicated soil ECe in UB was significantly different from all burned hillslopes ($p= 3.66x10^{-5}$) and B-15 was significantly different from B-08 ($p= 0.008$) and slightly different than B-04/08 ($p= 0.06$); B-08 and B-04/08 were not significantly different in measured ECe. UB was significantly different in bulk soil organic matter (OM) from B-15 ($p= 0.037$). All other comparisons of means were not significantly different.

Table 3. Mean ± S.E. bulk soil properties from top 30cm of soil profile (N=12 per plot) and unsaturated soil water retention model parameters from repacked composite samples (N=2 per plot).

| | Bulk Soil Properties+ | | | | | | Retention Curve Parameters* | | | |
|---|---|---|---|---|---|---|---|---|---|---|
| Field Plot | Clay (%) | Sand (%) | Porosity | Bulk Density ($g/cm^3$) | ECe ($mSm^{-1}$) | OM (%) | $\theta_r$ | $\theta_s$ | $\alpha$ | *n* |
| UB | 10.9 ±0.73[a] | 79.39 ±1.2[a] | 0.63 ±0.07[a] | 0.98 ±0.19[a] | 2.17 ±0.25[a] | 15.34 ±1.1[a] | 0.000 | 0.622 | 0.0592 | 8.940 |
| B-08 | 5.80 ±0.75[a] | 75.45 ±0.92[a] | 0.52 ±0.02[ab] | 1.26 ±0.05[ab] | 0.93 ±0.07[bc] | 8.68 ±0.49[ab] | 0.050 | 0.555 | 0.0592 | 7.258 |
| B-04/08 | 5.12 ±0.96[a] | 75.67 ±0.92[a] | 0.51 ±0.02[ab] | 1.28 ±0.06[ab] | 1.06 ±0.05[c] | 9.32 ±0.56[ab] | 0.038 | 0.534 | 0.0239 | 7.578 |
| B-15 | 5.69 ±0.85[a] | 78.45 ±0.92[a] | 0.49 ±0.02[b] | 1.35 ±0.06[b] | 1.46 ±0.13[b] | 8.21 ±0.50[b] | 0.000 | 0.503 | 0.0275 | 2.595 |

+ Values sharing the same letter are not statistically different

* Parameters for the van Genuchten model of soil-water retention developed using the Hyprop. Values are an average of two trials. θr is residual soil water content, θs is saturated soil-water content, and α and n are the van Genuchten parameters.

## 3.2 Soil Water Infiltration and Retention

Infiltrometer measurements of saturated hydraulic conductivity $K_{sat}$ and subsequent analysis of variance conclude there is a statistically significant difference ($p= 0.013$ ) among the research

plots in the summer of 2016 (Fig. 5). However, because all $K_{sat}$ measurements are on the same order of magnitude, they are considered not significantly different in practice. 2016 $K_{sat}$ means were 0.001±0.000 cm/s in UB, 0.006±0.007 cm/s in B-15, 0.001±0.002 cm/s in B-08, and 0.004±0.005 cm/s in B-04/08. In 2017 $K_{sat}$ means generally decreased to 0.001±0.002 cm/s in UB and B-15; and 0.001±0.001 cm/s in B-08 and B-04/08 and there is no statistically significant difference among plots.

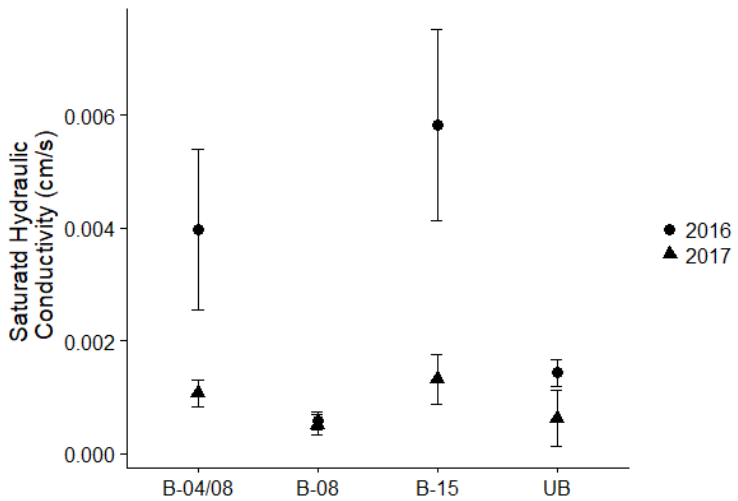


Figure 5. Saturated hydraulic conductivity per field plot. Points are the spatial mean (N=15 per year and plot) for the respective year and plot. Bars are the standard error.

Results from the Hyprop (with n= 2 per research plot) suggest some hypotheses, however the small sample size prohibits quantitative conclusions. The unsaturated soil water retention data from the Hyprop experiments (Figure 6), and the van Genuchten model best-fits to that data (Table 3), seemed to indicate differences in water retention among the field plots; however, there is not enough data to thoroughly test a quantitative difference in soil water retention properties between the different burned hillslopes (n=2 per plot). From the preliminary data, it seems that maximum, or saturated, soil water content may decrease with decreasing time since the most recent burn (UB > B-08 ≈ B-04/08 > B-15; as with porosity in Table 3). UB may have the most

plant available water (Table 4). Of the burned hillslopes, B-08 was most similar to the unburned reference. Differences in soil water content may be more notable among plots at the extremes, near field capacity ($\Psi_f$ = -33kPa) and the permanent wilting point ($\Psi_w$ = -15000kPa), with B-15 having the lowest volumetric water content throughout the range of matric potential (Figure 6). These statements remain hypotheses at present, however, due to the small sample size per plot.

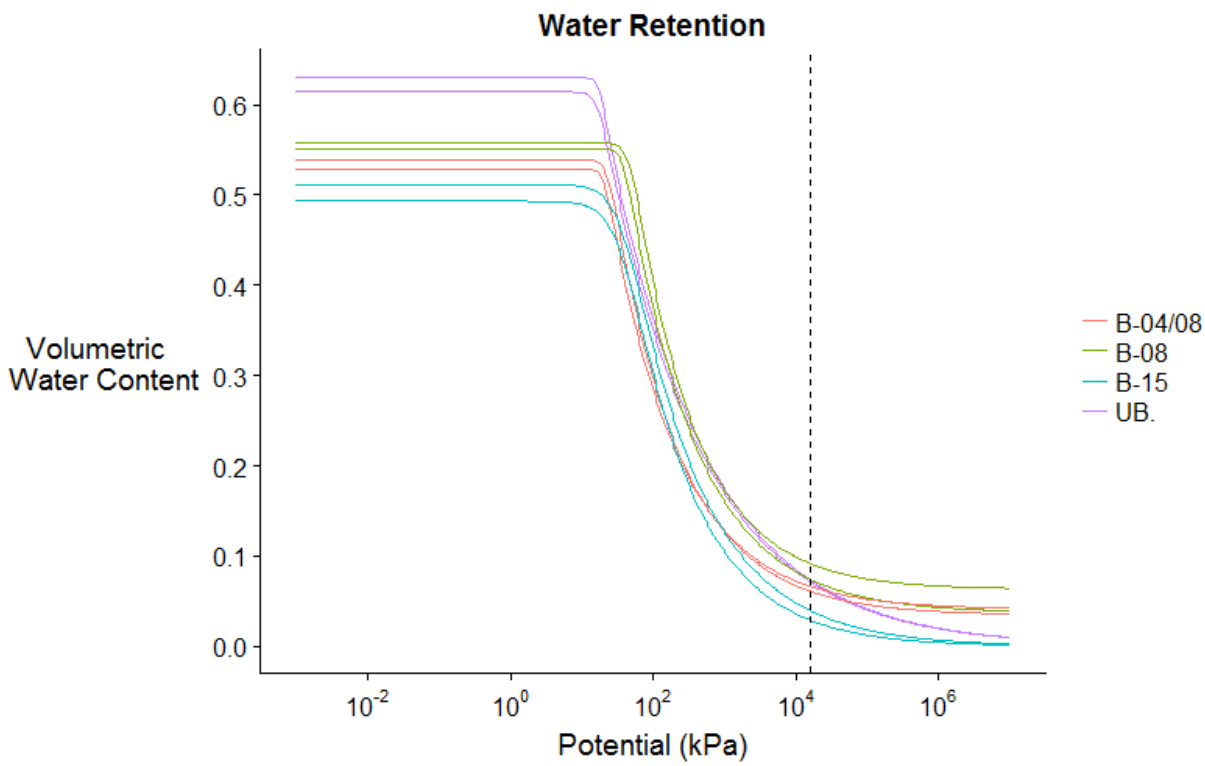


Figure 6. van-Genuchten soil water retention curves for two replicate composite soil samples from the top 30cm of each plot; Y-axis is volumetric water content and X-axis is matric potential.

3.3 Soil Moisture Monitoring:

A Kruskal-Wallis rank sum test performed on the soil moisture sensors, monitored throughout the dry season at depth of 15cm, indicated there was a significant difference ($p = 0.027$) in volumetric water content at the start of the dry season. UB started the dry season with much lower volumetric water content ($\theta$) than all burned hillslopes (Fig. 7). All burned hillslopes had $\theta$

≈ 0.2 at the start of the study period while the reference began with θ ≈ 0.13. The records began around the time of snow disappearance and after discharge from the White Salmon watershed had just begun to decline for the summer (Fig. 2). As the soils dried, UB lost soil moisture at a slower rate than the burned sites. B-15 and B-04/08 followed similar drying trends while B-08 remained slightly wetter through the dry season.

With very little summer rain, all plots reached a minimum soil moisture well below the permanent wilting point ($\Psi_w$ = -15000kPa) in the first week of August (Fig. 7). We computed each soil's minimum days of available water (mDAW) at 15cm depth as the time, in days, it took to reach permanent wilting point from the start of the study (shortly after complete snowmelt). Average mDAW is presented in Table 4. In addition to calculating the mDAW, we fit an exponential function defined as

$$\theta = FC * e^{\lambda t} \quad (3)$$

Where θ is volumetric water content, FC is the field capacity taken from Table 4, λ is the decay constant, and *t* is time in days. We then compared λ across all study plots. A Kruskall-Wallis rank sum test provided some evidence of a significant difference in the drying rate ($p = 0.079$) with the UB soil significantly different than all burned soils. The drying rates of burned soils were not significantly different from each other.

Table 4. Volumetric water content at field capacity ($\Psi_f$= -33kPa), wilting point ($\Psi_{wp}$= -15000kPa), and the plant available water (water fraction by volume) for each plot determined using Hyprop results. Days of available water is a minimum estimate, from the start of the study to the occurrence of wilting-point soil moisture levels. Decay Constant (λ) is the mean ± S.E. decay rate of all probes within a plot determined using equation 3.

| | Volumetric water content at: | | Date in 2017: | | | |
|---|---|---|---|---|---|---|
| Plot | Field Capacity | Permanent Wilting Point | Permanent Wilting Point | Plant available water | Days of available water | Decay Constant (λ) |
| UB | 0.248 | 0.073 | 07/01 | 0.176 | ≥ 15 | -0.047± 0.003* |
| B-08 | 0.249 | 0.083 | 07/04 | 0.166 | ≥ 18 | -0.066± 0.004 |
| B-04/08 | 0.188 | 0.064 | 07/03 | 0.125 | ≥ 17 | -0.070± 0.003 |
| B-15 | 0.193 | 0.034 | 07/15 | 0.158 | ≥ 29 | -0.076± 0.007 |

* Significantly Different

Soil moisture data collection at 50cm depth was limited by instrument malfunction. (Animals chewed on the wires, causing electrical connection problems.) The limited successful measurements at depth indicated that the soils at 50cm were consistently wetter than the soils at 15cm. Soil moisture at 50cm on all hillslopes exhibited a less steep drying curve in the early part of the dry season, and the burned hillslopes had elevated θ compared to the unburned reference. B-08 had the highest soil moisture at both 15cm and 50cm early in the dry season and UB, the lowest (Fig. 7).

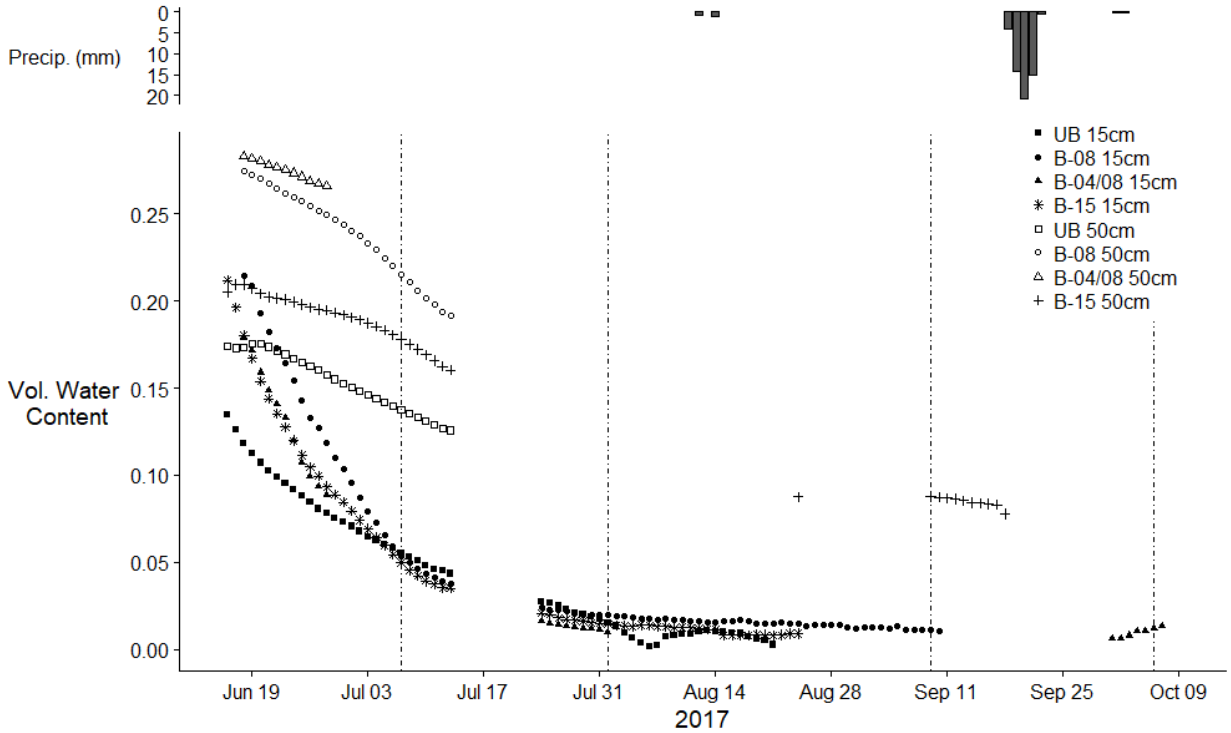


Figure 7: Daily soil moisture drydown during the summer dry season. Precipitation was almost entirely absent during the season (top). For field measurements of volumetric water content (θ) over time, solid symbols represent probes placed at a depth of 15cm and hollow symbols represent probes placed at 50cm. Each point is a daily average of four probes recording at 30 min intervals (N=192 per point). Vertical dashed lines are the dates of field surveying and geophysical EMI data collection.

## 3.4 Apparent Conductivity

The apparent soil electrical conductivity, a proxy for soil moisture, changed very little from July to September across all hillslopes in the near-surface 0-30cm depth interval ($\sigma_1$, Fig. 8A). We computed omni-directional semivariograms to interpret the possibility of spatial autocorrelation of ECa within each research plot and found that there was no significant autocorrelation (see appendix), i.e., ECa was unstructured and spatially random at the scale of this study (Webster and Oliver, 2007). We therefore used the spatial mean for statistical analyses. Early in the dry season, from July to August, the change in mean $\sigma_1$ ranged among the four plots from +0.337 to −0.509 mS m$^{-1}$ month$^{-1}$ ($\Delta\sigma = \sigma_{Aug} - \sigma_{Jul}$). A positive change (+$\Delta\sigma$) suggested increasing soil

moisture content and a negative change (-Δσ) decreasing soil moisture content in the 0-30cm depth interval. In the deeper soil interval at 30-50cm depth, early season soil moisture declined in three of the four plots ($\sigma_2$, Fig. 8B), at rates from -0.151 to -0.509 mS $m^{-1}$ $month^{-1}$. With the return of autumn precipitation between September and October, three of the four plots increased in soil moisture at both depths. The exception was B-04/08 fires, with notable changes at both depths of $\Delta\sigma_1$ = -0.719 mS $m^{-1}$ $month^{-1}$ and $\Delta\sigma_2$ = -3.867 mS $m^{-1}$ $month^{-1}$. Apparent soil moisture in UB was consistently high at 0-30cm, at which depth it increased from September to October, but low at 30-50cm, at which depth it did not significantly change over the dry season.

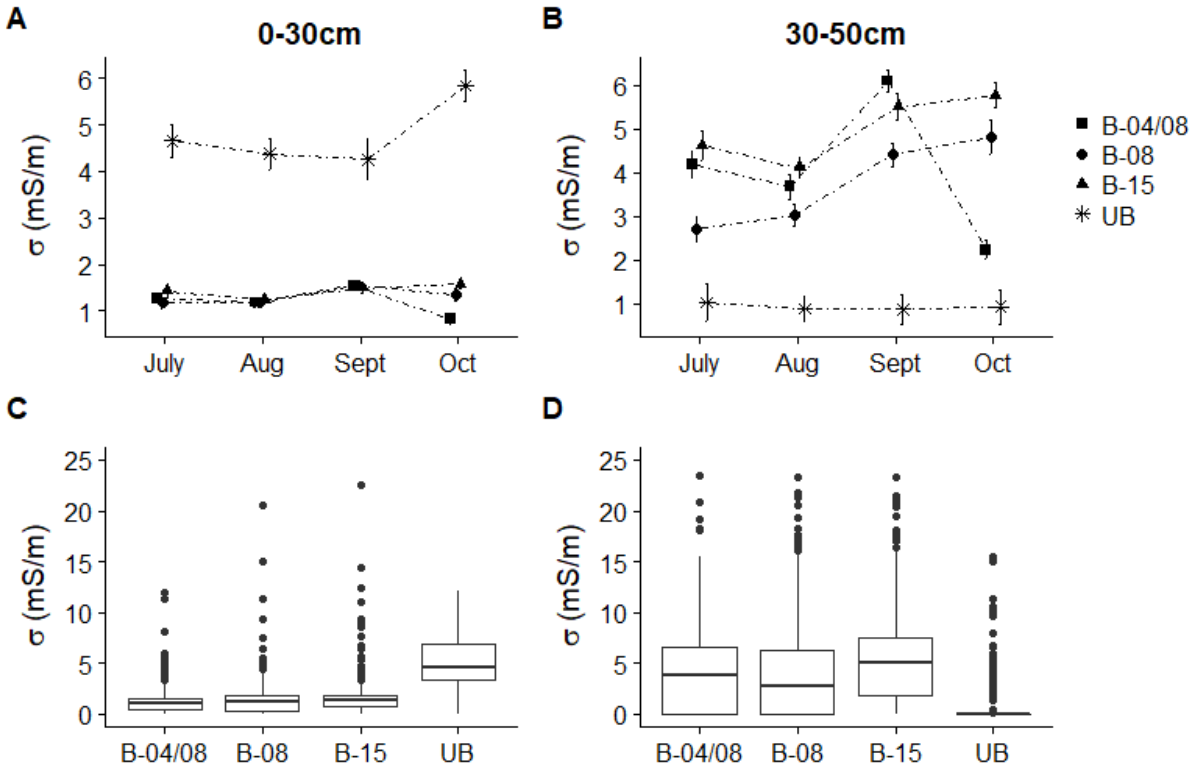


Figure 8. (A-B) Spatial average of soil apparent electrical conductivity (σ) for the 0-30cm ($\sigma_1$) and 30-50cm ($\sigma_2$) soil layers over the 2017 dry season. Points and whiskers are the mean ± S.E. N ~ 845 for all burned plots and N ~ 260 for the unburned reference. (C-D) Boxplot summary of overall dry season σ and comparison among plots for the 0-30cm ($\sigma_1$) and 30-50cm ($\sigma_2$) soil layers. N~ 3380 for all burned plots and N~ 1040 for the unburned reference. The box ends represent the 25th and 75th percentile, dark bar the median, whiskers the 10th and 90th percentiles, and points outliers.

Given the modest temporal changes in ECa, we examined differences among plots after combining the data from all dry-season months (Fig. 8 C&D). In general, UB was higher and more variable in apparent conductivity than all three burned hillslopes at 0-30cm, while the reverse was true for apparent conductivity at 30-50cm. Spatial measurements of apparent conductivity were not statistically different among the burned hillslopes. All burned hillslopes were significantly different than UB at both depths ($p= 2.2x10^{-16}$).

Given the contrasts in apparent conductivity in the shallow 0-30cm and deeper 30-50cm soil layers, we calculated $\Delta\sigma = \sigma_2-\sigma_1$ at each grid point of each plot. A positive vertical difference ($+\Delta\sigma$) indicated more deeper soil moisture and a negative difference ($-\Delta\sigma$) more shallow moisture. We performed a t-test to determine if the mean vertical difference among the EMI survey points within each plot was significantly different from 0. From the results of the t-test (Table 5), we determined there was no significant vertical moisture gradient in UB in any month of the study but that all burned plots had a statistically significant gradient of increasing moisture content with depth between the 0-30cm and 30-50cm soil layers.

Table 5. Average vertical difference in layer-electrical conductivity between 0-30cm and 30-50cm soil layers (Δσ) for each plot in each dry-season month and p-values with 95% confidence intervals for t-tests of vertical difference being significantly different from zero (H0: μ=0).

| | UB | | | B-08 | | | B-04/08 | | | B-15 | | |
|---|---|---|---|---|---|---|---|---|---|---|---|---|
| Month | Δσ | CI | P-value | Δσ | CI | P-value | Δσ | CI | P-value | Δσ | CI | P-value |
| Jul. | 2.51 | (-2.51, 7.54) | 0.287 | 5.43 | (3.98, 6.87) | 5.16E-11 | 5.98 | (4.92, 7.04) | 2.20E-16 | 8.25 | (6.05, 10.45) | 1.63E-11 |
| Aug. | -0.66 | (-2.48, 1.15) | 0.438 | 3.94 | (3.02, 4.85) | 9.90E-14 | 6.47 | (4.65, 8.30) | 1.74E-10 | 4.53 | (4.00, 5.06) | 2.20E-16 |
| Sep. | 0.87 | (-1.69, 3.42) | 0.458 | 5.72 | (4.25, 7.18) | 2.75E-12 | 6.63 | (5.95, 7.31) | 2.20E-16 | 7.93 | (6.52, 9.34) | 2.20E-16 |
| Oct. | 0.07 | (-3.28, 3.41) | 0.964 | 9.17 | (7.44, 10.91) | 2.20E-16 | 5.03 | (4.09, 5.97) | 2.20E-16 | 6.58 | (5.84, 7.32) | 2.20E-16 |

## 3.5 Surface Cover

A summary of the composition of living vegetation for each plot is presented in Figure 9A. UB's surface cover mostly consisted of shade-tolerant forbs and herbs due to an intact forest canopy consisting of *Abies amabilis* and *Tsuga mertensiana*. As expected, UB had the highest percentage of live tree cover by basal area (Fig. 9B), with several large trees (diameter at breast height > 120cm) throughout the research plot. The duff layer ranged from 2-4cm thick in UB. B-08 and B-04/08 were dominated by graminoids and forbs/herbs rather than trees or shrubs. However, B-04/08 was higher in graminoid cover and B-08 was higher in forb/herb cover. B-15 had the highest abundance of bare soil area and shrub cover and was lowest in total area covered in all other categories. B-08 had the second most live trees (after UB) with approximately 6 live tree saplings, while B-04/08 had the lowest at 2. There were 4 live saplings in B-15.

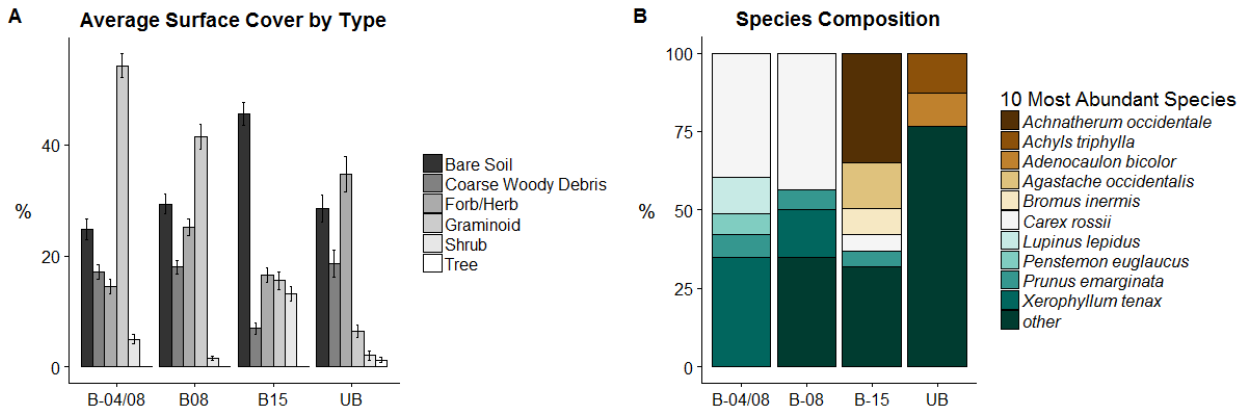


Figure 9. (A) Average percent abundance of each surface cover for all plots. Whiskers represent the S.E. (B) Average species composition of 10 most abundant species for all sites. Bars represent the percentage of each abundance class for the respective surface cover type.

To assess possible spatial relations between surface cover and soil moisture, we calculated the mean and standard deviation of the soil electrical conductivity in each soil layer (σ) within each surface cover type and relative abundance category (Fig. 10). This analysis revealed slight differences in the relationships of different surface covers with soil moisture (by σ proxy) at both depths. Under most cover types, σ was significantly higher in the 30-50cm layer compared to the shallower 0-30cm layer. Under bare soil, soil moisture in the 30-50cm layer showed little variability with the intensity of the overlying bare cover, but moisture content (by $\sigma_1$ proxy) in the 0-30cm layer increased until the abundance of bare soil reached 50% cover, after which it gradually decreased in magnitude. Under coarse woody debris, forb/herb cover, and live trees (young or mature), soil moisture decreased with cover abundance in the 30-50cm layer but increased with abundance in the 0-30cm layer. The reverse was true for graminoid and shrub cover.

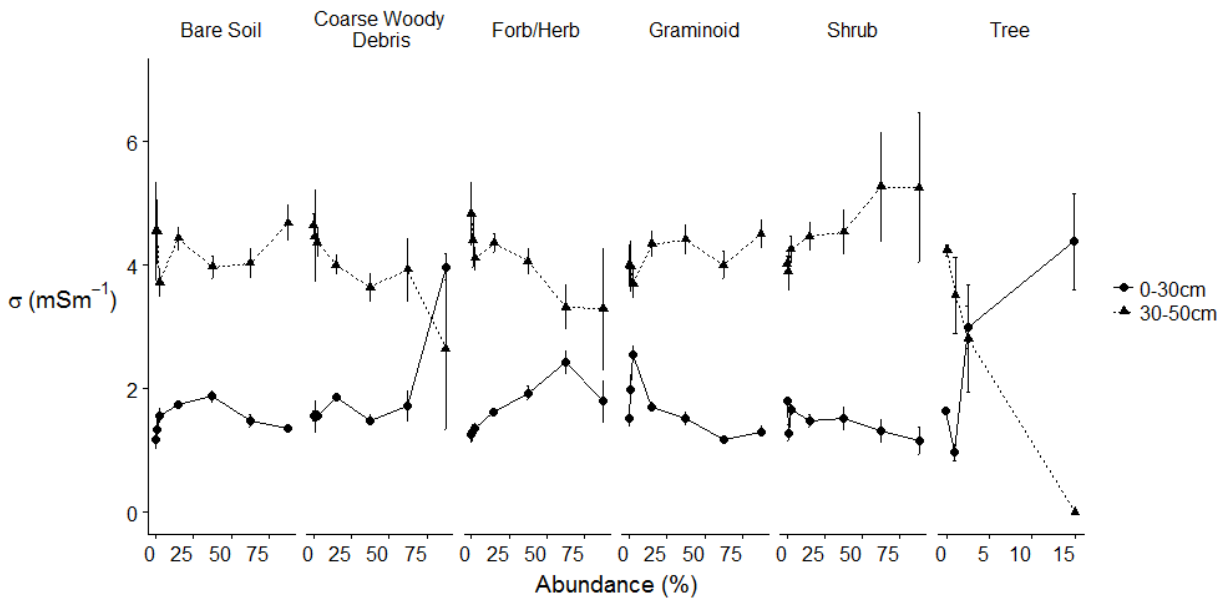


Figure 10. Average apparent soil electrical conductivity in the discrete shallow and deeper soil layers (σ) for each cover type across its different degrees of abundance. Points represent the mean ± S.E. of σ, a proxy for soil moisture content, with σ data pooled across all plots and survey months.

In the 0-30cm layer, σ was markedly highest under areas with >75% coarse woody debris (mean 3.98 mS m$^{-1}$) and under areas with >15% tree cover (mean 4.38 mS m$^{-1}$). Under these same cover categories, σ in the 30-50cm layer was lowest (mean 2.65 mS m$^{-1}$ and 0.00 mS m$^{-1}$, respectively).

## 4. Discussion

### 4.1 Persistence of Wildfire Influences on Bulk Soil and Hydraulic Properties

The three fire-affected hillslopes were comparable in porosity, texture, electrical conductivity, and organic matter. Although soils differed slightly in salinity, all were less than 3 $mSm^{-1}$, were classified as nonsaline, and did not significantly influence EMI results. However, there was an observable difference between burned soils and the unburned reference soil, with increased bulk density and decreased porosity within the burned soils. This finding is consistent with other field studies. Andreu et al. (2001) reported decreases in soil bulk density in a mountainous region of southern Spain after wildfire and Pierson et al. (2001) had similar findings in a fire-affected watershed in Nevada. Stoof et al. (2010) measured increases in bulk density after simulated soil burning in laboratory experiments. Alterations in bulk density and porosity are the product of reduced aggregate stability (Brady and Weil, 2010). The destabilization of soil aggregates resulted from the combustion and removal of soil organics that hold soil structures together (DeBano et al., 1998). When saturated with water after the removal of soil organic material (i.e., during autumn precipitation following wildfire), the soil structure collapses, decreasing the pore space and increasing bulk density (Hillel, 1982). This then leads to soil surface sealing, and eventual increased runoff during high intensity rains (Debano et al., 1998). Interestingly, the soils affected by two burns (in 2004 and 2008) were slightly higher in bulk density than the soils affected by only the 2008 fire. From this observation, we hypothesize that recurrent fires may lead to highly compacted soils more susceptible to increased runoff and erosion. Given the similarities among burned hillslopes, there is no evidence to suggest the soils last burned in 2008 have recovered hydrologically any better than those burned in 2015, and so it may take substantially longer (>10 yrs) to do so in this semi-arid ecosystem.

From the soil moisture sensors, we observed volumetric water content measured at 15cm depth in the unburned reference hillslope near the start of the dry season (Figure 7) was substantially less than that in the burned hillslopes but the burned hillslopes were all similar. All plots began the study at or below their respective field capacities, which may be due to the relatively high hydraulic conductivities (Figure 5) preventing the soils from reaching saturation at any given time. If the soils in all plots may never fully saturate, the highest water content we can expect is field capacity. Because the reference hillslope was situated near the top of a knoll, but low enough to achieve comparable slope, differences in soil moisture may be the consequence of differences in up/down slope moisture distribution. In early spring, the unburned plot experiences abundant water inputs from snowmelt and is freely drained. The lower moisture content near the surface in the unburned site may be the result of a higher rate of shallow, early-season transpiration in combination with rapid drainage (Adams et al., 1991). Trees and taller understory vegetation may have begun transpiration before snowmelt is completed. After snowmelt is complete, the water supply is then cut off and water use may shift to capillary conditions, drawing water from deeper soil layers. During the early summer, soil water availability is then dominated by evapotranspiration. In late summer, when soil water is at its minimum, understory transpiration in the unburned plot may shut down. If transpiration does not resume with the return of autumn precipitation, soil water conditions are controlled by infiltration. The burned plots may experience a similar trend in the soil water budget, but with slight shifts in evapotranspiration. All burned plots likely experience reduced evapotranspiration due to less perennial vegetation after wildfire which may also have helped promote higher early-season water contents in burned soils; this was observed in a southwestern US semi-arid

catchment by Poon and Kinoshita (2018). Although the reference hillslope began the dry season with less soil moisture near the surface, the moisture was depleted through the dry season at a less rapid rate than in the burned hillslopes. We attribute this observation to a lower evaporation and soil temperatures at the reference hillslope compared to the burned hillslopes. The presence of an intact canopy seems to keep the forest floor cooler than the exposed soil found at all burned sites (Supplemental fig. 5). Without shade and significant protection from wind, there will be a high evaporative demand on the burned hillslopes. Because the majority of plants in these burned plots are shallow rooting, with an approximate rooting depth of about 30cm, early summer soil moisture is less likely to be amended through capillary transport from deeper soil layers. Trends in early autumn soil moisture of the twice-burned plot appeared to diverge from that of a single burn plot, suggesting there may be another governing process working in parallel with infiltration. While this is restricted to the conditions of our research site with a unique burn history, it is an important observation that warrants further investigation.

Another factor potentially contributing to the rapid loss of soil moisture at the field site is that wildfires are known to reduce soil water retention through loss of organic matter, increased bulk density, and fire-induced hydrophobicity (Ebel 2012; Stoof et al. 2010). Our analysis using the Hyprop seems to suggest this is a possibility for our soils, as retention generally decreases with increasing bulk density (Fig. 6). The combustion of organic matter, reduced aggregate stability, and soil compaction reduces the water holding capacity of burned soils (Stoof et al., 2010). Often, these reductions are most notable at lower tensions. Higher organic matter content and lower bulk density in the unburned reference resulted in higher observed water content most tension values and allowed the soil to release moisture at a slower rate than the burned soils, as

was observed by our soil moisture probes (Fig. 7, Table 4). Compaction of the burned soils (increased bulk density), after being saturated, likely reduced the volumetric water contents lower tensions. Our observations suggest wildfires reduce the total amount of water capable of being stored in the soil and that short-interval recurrent fires may have compounding effects. Reductions to water holding capacity consequently lead to shifts in the water cycle. More water is diverted from the "green" water cycle (water available to plants in the vadose zone) to the "blue" water cycle (water stored in surface water bodies and groundwater systems). Reductions to soil water storage also increase the duration of drought-stress during the summer dry season.

### 4.2 Post-wildfire Soil Moisture Variations in Space and Time

Electromagnetic induction (EMI) surveys, constrained to discrete-layer values of soil electrical conductivity (σ), were used as a proxy for variation in soil moisture through time and across plots. Surprisingly, there was no spatial autocorrelation in σ (i.e., no smooth spatial structure to the signal) in any of the plots during any month of the study, suggesting that the spatial distribution of σ values was relatively random in the shallow subsurface. Low σ near the surface (0-30 mS $m^{-}$) in all plots and during all dry season months (July-October) was consistent with low water contents measured by moisture probes and the overall dry state of the sites. Slight differences in σ between burned and unburned hillslopes revealed distinct changes to soil water content and its distribution with depth. There was a strong vertical gradient in soil moisture at all burned hillslopes and in all months of the study, with drier soils near the surface (0-30cm) and wetter soils deeper in the profile (30-50cm). There was no significant vertical gradient in moisture detected in the unburned reference hillslope, suggesting a relatively uniform vertical distribution of soil moisture from 0-50cm. We hypothesize the vertical gradient in soil moisture

present in the burned sites is the consequence of high evaporative demand from increased soil temperatures and exposure to wind upon loss of the forest canopy and vegetative cover. Combustion of roots may also lead to preferential flow pathways, enabling rapid infiltration and subsequent storage deeper in the soil profile. The stability of this vertical gradient in soil moisture suggests the bulk of evapotranspiration is limited to the top 30cm of soil. These observations indicate evaporation and soil temperature are key factors limiting soil moisture contents at the surface after wildfire, but moisture can be retained in deeper soil layers beneath severely burned areas through the dry season.

The relatively constant ECa in B-08 and B-15 from September to October may suggest a process that restricts infiltration during the transition from dry to wet seasons. We hypothesize this results from a combination of increased soil compaction, hyper-dry conditions, and residual hydrophobicity leading to infiltration excess overland flow. This was unexpected as hydrophobicity is generally considered to be short-lived, typically weakening within 3-4 months after fire (Huffman et al. 2001) and becoming undetectable 1-2 years after fire (MacDonald and Huffman 2004). If hydrophobicity remains present in the burned sites, the observed vertical gradient in ECa from September to October in all burned sites may suggest the hydrophobic layer in this type of Cascade Montane system is spatially discontinuous. An incomplete hydrophobic layer allows water to infiltrate into the soil by preferential flow through voids in the soil profile created by the combustion of tree stumps and roots. This is expected as the hydrophobic layer is rarely spatially intact (Mataix-Solera and Doerr 2004, DeBano 2000). The dramatic decrease in ECa from September to October in B-04/08 (Fig. 7A&B) may indicate a combination of infiltration inhibiting processes and a sudden shift in transpiration.

## 4.3 Surface Cover is Dependent on Underlying Apparent Conductivity

From 2016 and 2017 vegetation and surface cover surveys, we identified distinct differences among all plots. As expected, B-15 was highest in bare soil surface and lowest in coarse woody debris. This may be because the plot has had the least amount of time to recruit seedlings and any leftover fuel remains as snags and standing dead trees. B-04/08 was least diverse in its species composition, consisting mostly of *Carex rossii*. The low species diversity may suggest the two short-interval fires may have significantly reduced the seedbank or greatly reduced the reproduction capacity of surviving plants. Surviving seeds and tubers could have sprouted after the 2004 fire only to be later consumed by the 2008 fire, as commonly found in areas affected by short interval fires (Diaz-Delgado et al. 2002, Johnstone and Chapin 2006).

The trend of increasing shallow (0-30cm) soil moisture content (by σ proxy) with relative abundance of coarse woody debris suggests evaporation of water from the top 30cm is suppressed due to shading or obstruction of the soil surface. Overlying coarse woody debris may also limit infiltration of snowmelt deeper into the soil profile, accounting for the inverse trend deeper in the profile (30-50cm depth). This may also indicate that, during the dry season, soil moisture at the surface is highly dependent on vapor deposition during pre-dawn and subsequent evaporation mid-day. Areas beneath coarse woody debris are well shaded throughout the day, reducing soil temperatures and soil water evaporation. Decreasing soil moisture in the 0-30cm depth interval with increasing abundance of small shrubs and graminoids and decreasing moisture in the 30-50cm interval with increasing abundance of trees may reflect moisture depletion in the root zones, with trees accessing deeper water stores than shrubs and graminoids.

Alternatively, this could indicate that slightly higher water contents at depth are enabled, despite moisture loss by plant uptake, perhaps by improved permeability and macropore flow within the root zone in soils vegetated by shrubs and graminoids (more so than by forbs/herbs). Under any cover type in the burned areas, though, the strong and persistent vertical gradient in soil moisture means that there is the potential for surviving deeper rooting shrubs and trees, or even perennial graminoids or herbs/forbs, to participate in hydraulic redistribution of water from lower soil depths to shallower layers (Brooks et al., 2002; Meinzer et al., 2004), and so aid in post-fire seed germination and ecosystem recovery.

The very rapid declines in soil moisture observed by this study in all burned hillslopes early in the dry season likely increases the susceptibility for fire recurrence at these locations. It is widely accepted that forests exposed to drought and water-stressed conditions experience elevated risk of seedling mortality and insect outbreaks such as *Dendroctonus ponderosae* and *Choristoneura freeman* (Allen et al., 2010; Van Mantgem et al., 2009). After snowmelt, there is a prolific growth of understory vegetation within the first few weeks, and the newly sprouted vegetation eventually dries out during the summer drought. This combination of over-abundant fuel and low soil moisture is indicative of high wildfire risk (Waring and Coops 2016).

## 5. Conclusion

To understand how wildfires and primary succession affect soil water availability across a fire-altered landscape, we compared the magnitude and time-dependency of soil moisture across a gradient varying burn histories. We used both continuous measurements of soil moisture at depths of 15cm and 50cm and periodic electromagnetic induction surveys to assess how subsurface moisture dynamics differ between burn histories. Our study is novel in that we apply electromagnetic induction to a new setting to collect a large amount of three-dimensional spatially distributed soil data and in that we begin to explore potential impacts of recurrent fire on the hydrologic cycle. From the data collected at these few sites, it seems that our research suggests soil moisture and drying patterns are relatively indistinguishable between recently burned (within 10 years) hillslopes of varying recovery time (2 vs 9 years undisturbed). Soils affected by recurrent wildfire were also indistinguishable from those affected by single fire events during the summer drought period but show signs of variation during seasonal transitions. This may suggest short interval recurrent wildfires, or fires occurring over the same soil surface less than 10 years apart, have compounding impacts on the hydrologic cycle in this region. We might expect these observations to significantly differ in wetter systems on the windward side of mountains or on north facing slopes due to a higher water flux. In drier systems with less water flux on the rainshadow side of mountains, our observations may be more applicable as they were collected during a summer drought period.

Our study also demonstrates the importance of water as a limiting resource for vegetative regrowth. The concentration of dense plant cover near coarse woody debris and association with areas of high apparent conductivity indicate vegetation is preferential to areas with higher

moisture contents. After a fire disturbance, re-colonizing species are likely to germinate in areas with the highest soil water content. In the absence of a recurrent fire, and if these species are able to survive the summer drought, they may then promote moisture redistribution. This consequently increases the spatial coverage and duration of plant available water. Leading to dense patches of vegetation that facilitate their own moisture needs through shading of the soil surface and lifting water from deeper soil horizons.

There remains a need for further research in understanding soil moisture and vadose zone hydrology in fire-disturbed landscapes. Most studies have focused on single fire events and catchment-scale responses; few have examined the effects of recurrent fire on hillslope hydrology and vadose zone processes. Our study reveals that soil moisture variability is relatively indistinguishable during the dry season in burn areas regardless of their most recent fire or fire frequency, at least for Cascades montane forests affected by wildfire within the past 10 years. However, we provide evidence to suggest there is a distinct difference between areas affected by recurrent fire and those affected by a single fire during the transition from dry to wet seasons. Future studies can further increase our understanding of the consequences of recurrent fire. As drought risk, fire occurrence, and climate change continues, there is a greater need to understand how landscapes are adapting to significant disturbances.

Works Cited

Abbott LB, Roundy BA. Available water influences field germination and recruitment of seeded grasses. Journal of Range Management. 2003 Jan 1:56-64.

Abdu H, Robinson DA, Seyfried M, Jones SB. Geophysical imaging of watershed subsurface patterns and prediction of soil texture and water holding capacity. Water resources research. 2008 Apr 1;44(4).

Adams PW, Flint AL, Fredriksen RL. Long-term patterns in soil moisture and revegetation after a clearcut of a Douglas-fir forest in Oregon. Forest Ecology and Management. 1991 Jul 16;41(3-4):249-63.

Agee. Fire ecology of Pacific Northwest forests. Island press. 1996.

Alauzis MV, Mazzarino MJ, Raffaele E, Roselli L. Wildfires in NW Patagonia: long-term effects on a Nothofagus forest soil. Forest Ecology and Management. 2004 May 6;192(2):131-42.

Allen CD, Macalady AK, Chenchouni H, Bachelet D, McDowell N, Vennetier M, Kitzberger T, Rigling A, Breshears DD, Hogg ET, Gonzalez P. A global overview of drought and heat-induced tree mortality reveals emerging climate change risks for forests. Forest ecology and management. 2010 Feb 5;259(4):660-84.

Andreu V, Imeson AC, Rubio JL. Temporal changes in soil aggregates and water erosion after a wildfire in a Mediterranean pine forest. Catena. 2001 May 18;44(1):69-84.

Attiwill PM. The disturbance of forest ecosystems: the ecological basis for conservative management. Forest Ecology and management. 1994 Feb 1;63(2-3):247-300.

Lombao A, Barreiro A, Cancelo-González J, Matín A, Díaz-Raviña M. Impact of termal shock on forest soils affected by fires of different severity recurrence. Span. J. Soil Sci. 2015;5(2):165-79.

Bladon KD, Emelko MB, Silins U, and Stone M. Wildfire and the Future of Water Supply. Environmental Science & Technology 2014 48 (16), 8936-8943

Braun-Blanquet J. Plant sociology. The study of plant communities. Plant sociology. The study of plant communities. First ed. 1932.

Brooks JR, Meinzer FC, Coulombe R, Gregg J. Hydraulic redistribution of soil water during summer drought in two contrasting Pacific Northwest coniferous forests. Tree physiology. 2002 Nov 1;22(15-16):1107-17.

Bixby RJ, Cooper SD, Gresswell RE, Brown LE, Dahm CN, Dwire KA. Fire effects on aquatic ecosystems: an assessment of the current state of the science. Freshwater Science. 2015 Dec 1;34(4):1340-50.

Boisramé G, Thompson S, Stephens S. Hydrologic responses to restored wildfire regimes revealed by soil moisture-vegetation relationships. Advances in Water Resources. 2018 Feb 1;112:124-46.

Brady NC, Weil RR. Elements of the nature and properties of soils. Upper Saddle River, NJ: Pearson Educational International; 2010.

Brus DJ, Heuvelink GB. Optimization of sample patterns for universal kriging of environmental variables. Geoderma. 2007 Feb 15;138(1):86-95.

Callegary JB, Ferré T, Groom RW. Vertical spatial sensitivity and exploration depth of low-induction-number electromagnetic-induction instruments. Vadose Zone Journal. 2007 Feb 1;6(1):158-67.

Cerdà A. Fire effects on soils and restoration strategies. CRC Press; 2009 Jan 5.

Cerdà A, Robichaud P. Fire effects on soil infiltration. Fire effects on soils and restoration strategies. Science Publishers, New Hampshire. 2009 Jan 5:81-103.

Certini. 2005. Effects of fire on soils. Oecologia. 143(1): 1-10.

Collins BM, Miller JD, Thode AE, Kelly M, Van Wagtendonk JW, Stephens SL. Interactions among wildland fires in a long-established Sierra Nevada natural fire area. Ecosystems. 2009 Feb 1;12(1):114-28.

Corwin DL, Lesch SM. Application of soil electrical conductivity to precision agriculture. Agronomy Journal. 2003 May 1;95(3):455-71.

Data Resources Management (DRM) and Fire and Aviation Management (FAM), Pacific Northwest Region, Forest Service, U.S. Department of Agriculture

DeBano LF. The role of fire and soil heating on water repellency in wildland environments: a review. Journal of Hydrology. 2000 May 29;231:195-206.

DeBano LF, Neary DG, Ffolliott PF. Fire effects on ecosystems. John Wiley & Sons; 1998 Mar 9.

Dennison PE, Brewer SC, Arnold JD, Moritz MA. Large wildfire trends in the western United States, 1984–2011. Geophysical Research Letters. 2014 Apr 28;41(8):2928-33.

Díaz-Delgado R, Lloret F, Pons X, Terradas J. Satellite evidence of decreasing resilience in Mediterranean plant communities after recurrent wildfires. Ecology. 2002 Aug 1;83(8):2293-303.

Doerr SH, Shakesby RA, Walsh R. Soil water repellency: its causes, characteristics and hydro-geomorphological significance. Earth-Science Reviews. 2000 Aug 31;51(1):33-65.

Doolittle JA, Brevik EC. The use of electromagnetic induction techniques in soils studies. Geoderma. 2014 Jul 31;223:33-45.

Duniway MC, Palmquist E, Miller ME. Evaluating rehabilitation efforts following the Milford Flat Fire: successes, failures, and controlling factors. Ecosphere. 2015 May 1;6(5):1-33.

Ebel BA. Wildfire impacts on soil-water retention in the Colorado Front Range, United States. Water Resources Research. 2012 Dec 1;48(12).

Franklin JF, Dyrness CT. Natural vegetation of Oregon and Washington. US Pacific Northwest Forest and Range Experiment Station. General Technical Report. PNW. 1973;8.

Franz TE, King EG, Caylor KK, Robinson DA. Coupling vegetation organization patterns to soil resource heterogeneity in a central Kenyan dryland using geophysical imagery. Water Resources Research. 2011 Jul 1;47(7).

Friedman SP. Soil properties influencing apparent electrical conductivity: a review. Computers and electronics in agriculture. 2005 Mar 31;46(1):45-70.

Gee GW, Or D. 2.4 Particle-size analysis. Methods of soil analysis. Part. 2002 Jan;4(598):255-93.

Harvey BJ, Donato DC, Turner MG. High and dry: post-fire tree seedling establishment in subalpine forests decreases with post-fire drought and large stand-replacing burn patches. Global Ecology and Biogeography. 2016. 25: 655-669.

Hatten J, Zabowski D, Ogden A, Theis W, Choi B. Role of season and interval of prescribed burning on ponderosa pine growth in relation to soil inorganic N and P and moisture. Forest ecology and management. 2012 Apr 1;269:106-15.

Hendrickx JM, Borchers B, Corwin DL, Lesch SM, Hilgendorf AC, Schlue J. Inversion of soil conductivity profiles from electromagnetic induction measurements. Soil Science Society of America Journal. 2002 May 1;66(3):673-85.

Hillel D. Introduction to soil physics. Academic press; 2013 Oct 22.

Hosseini M, Keizer JJ, Pelayo OG, Prats SA, Ritsema C, Geissen V. Effect of fire frequency on runoff, soil erosion, and loss of organic matter at the micro-plot scale in north-central Portugal. Geoderma. 2016 May 1;269:126-37.

Huffman EL, MacDonald LH, Stednick JD. Strength and persistence of fire-induced soil hydrophobicity under ponderosa and lodgepole pine, Colorado Front Range. Hydrological Processes. 2001 Oct 30;15(15):2877-92.

Johnstone JF, Chapin FS. Effects of soil burn severity on post-fire tree recruitment in boreal forest. Ecosystems. 2006 Feb 1;9(1):14-31.

Korosec MA. Geologic map of the Mount Adams quadrangle, Washington. Washington State Dept. of Natural Resources, Olympia (USA). Div. of Geology and Earth Resources; 1987 Jan 1.

Lesch SM, 2005. Sensor-directed response surface sampling designs for characterizing spatial variation in soil properties. Comput. Electron. Agric., 46:153-180

Lesch SM. Statistical software package for estimating field scale spatial salinity patterns from electromagnetic induction signal data ESAP v. 2.35. USDA-ARS. 2006.

Lesch SM, J.D. Rhoades, and D.L. Corwin. 2000. The ESAP Version 2.01r user manual and tutorial guide. Research Report #146. George E. Brown Jr., Salinity Laboratory, Riverside, CA, 153pp

Lesch SM, Corwin DL, Robinson DA. 2005. Apparent soil electrical conductivity mapping as an agricultural management tool in arid zone soils. Computers and Electronics in Agriculture. 46(1):351-78.

Loáiciga HA, Pedreros D, Roberts D. Wildfire-streamflow interactions in a chaparral watershed. Advances in Environmental Research. 2001 Aug 1;5(3):295-305.

MacDonald LH, Huffman EL. Post-fire soil water repellency. Soil Science Society of America Journal. 2004 Sep 1;68(5):1729-34.

Malkisnon D, Wittenberg L, Beeri O, Barzilai R. Effects of repeated fires on the structure, composition, and dynamics of Mediterranean maquis: short-and long-term perspectives. Ecosystems. 2011 Apr 1;14(3):478-88.

Mataix-Solera J, Doerr SH. Hydrophobicity and aggregate stability in calcareous topsoils from fire-affected pine forests in southeastern Spain. Geoderma. 2004 Jan 1;118(1-2):77-88.

Mayor AG, Bautista S, Llovet J, Bellot J. Post-fire hydrological and erosional responses of a Mediterranean landscpe: Seven years of catchment-scale dynamics. Catena. 2007 Sep 1;71(1):68-75.

McNeill JD. Electromagnetic terrain conductivity measurement at low induction numbers. Tech. Note TN-6. Geonics Ltd., Mississauga, ON. 1980.

McNeill JD, Bosnar M. Application of dipole-dipole electromagnetic systems for geological depth sounding. Tech. Note TN-31. Geonics Ltd., Mississauga, ON. 1999.

Meinzer FC, Brooks JR, Bucci S, Goldstein G, Scholz FG, Warren JM. Converging patterns of uptake and hydraulic redistribution of soil water in contrasting woody vegetation types. Tree Physiology. 2004 Aug 1;24(8):919-28.

Melgoza G, Nowak RS, Tausch RJ. Soil water exploitation after fire: competition between Bromus tectorum (cheatgrass) and two native species. Oecologia. 1990 May 1;83(1):7-13.

Moffett KB, Robinson DA, Gorelick SM. Relationship of salt marsh vegetation zonation to spatial patterns in soil moisture, salinity, and topography. Ecosystems. 2010 Dec 1;13(8):1287-302.

Moody JA, Martin DA. Post-fire, rainfall intensity–peak discharge relations for three mountainous watersheds in the western USA. Hydrological processes. 2001 Oct 30;15(15):2981-93.

Mora JL, Armas-Herrera CM, Guerra JA, Arbelo CD, Rodríguez-Rodríguez A, Notario del Pino JS. A Comparative Study of Long-Term Effects on Fire-Affected Volcanic Soils in Two Different Ecosystems in the Canary Islands. Land Degradation & Development. 2015 Jan 1.

Murphy JD, Johnson DW, Miller WW, Walker RF, Carroll EF, Blank RR. Wildfire effects on soil nutrients and leaching in a Tahoe Basin watershed. Journal of environmental Quality. 2006 Mar 1;35(2):479-89.

Neary DG, Klopatek CC, DeBano LF, Ffolliott PF. Fire effects on belowground sustainability: a review and synthesis. Forest ecology and management. 1999 Sep 13;122(1-2):51-71.

Olson DL, Agee JK. Historical fires in Douglas-fir dominated riparian forests of the southern Cascades, Oregon. Fire Ecology. 2005;1(1):50-74.

Omernik JM. Ecoregions of the conterminous United States. Annals of the Association of American geographers. 1987 Mar 1;77(1):118-25.

Pierson FB, Robichaud PR, Spaeth KE. Spatial and temporal effects of wildfire on the hydrology of a steep rangeland watershed. Hydrological processes. 2001 Oct 30;15(15):2905-16.

Poon PK, Kinoshita AM. Spatial and temporal evapotranspiration trends after wildfire in semi-arid landscapes. Journal of Hydrology. 2018 Apr 1;559:71-83.

PRISM Climate Group, Oregon State University, http://prism.oregonstate.edu, created 28 April 2018.

Rhoades JD, Raats PA, Prather RJ. Effects of liquid-phase electrical conductivity, water content, and surface conductivity on bulk soil electrical conductivity. Soil Science Society of America Journal. 1976;40(5):651-5.

Robbins CW and Wiegand CL. Field and laboratory measurements. Agricultural Salinity Assessment and Management. ASCE Manual. 1990; 71:203-219.

Robinson DA, Abdu H, Jones SB, Seyfried M, Lebron I, Knight R. Eco-geophysical imaging of watershed-scale soil patterns links with plant community spatial patterns. Vadose Zone Journal. 2008 Nov 1;7(4):1132-8.

Schindler U, Durner W, Von Unold G, Mueller L, Wieland R. The evaporation method: Extending the measurement range of soil hydraulic properties using the air-entry pressure of the ceramic cup. Journal of Plant Nutrition and Soil Science. 2010 Aug 1;173(4):563-72.

Schulte EE, Hopkins BG. Estimation of soil organic matter by weight loss-on-ignition. Soil organic matter: analysis and interpretation. 1996 :21-31.

Serrano JM, Shahidian S, Da Silva JR. Apparent electrical conductivity in dry versus wet soil conditions in a shallow soil. Precision Agriculture. 2013 Feb 1;14(1):99-114.

Schaap MG, Bouten W, Verstraten JM. Forest floor water content dynamics in a Douglas fir stand. Journal of Hydrology. 1997 Dec 20;201(1-4):367-83.

Shakesby RA. Post-wildfire soil erosion in the Mediterranean: review and future research directions. Earth-Science Reviews. 2011 Apr 30;105(3):71-100.

Sheets KR, Hendrickx JM. Noninvasive soil water content measurement using electromagnetic induction. Water resources research. 1995 Oct 1;31(10):2401-9.

Sherlock MD, McDonnell JJ. A new tool for hillslope hydrologists: spatially distributed groundwater level and soilwater content measured using electromagnetic induction. Hydrological Processes. 2003 Jul 1;17(10):1965-77.

Stoof CR, Wesseling JG, Ritsema CJ. Effects of fire and ash on soil water retention. Geoderma. 2010 Nov 15;159(3-4):276-85.

Smith HG, Sheridan GJ, Lane PN, Nyman P, Haydon S. Wildfire effects on water quality in forest catchments: a review with implications for water supply. Journal of Hydrology. 2011 Jan 5;396(1-2):170-92.

Soil Survey Staff, Natural Resources Conservation Service, United States Department of Agriculture. Official Soil Series Descriptions. Available online. Accessed May 16, 2018.

Tinker DB, Knight DH. Coarse woody debris following fire and logging in Wyoming lodgepole pine forests. Ecosystems. 2000 Sep 21;3(5):472-83.

USDA-FSA-APFO Aerial Photography Field Office, 20160111, FSA 10:1 NAIP Imagery 3.75 x 3.75 minute JPEG2000 from The National Map: USDA-FSA-APFO Aerial Photography Field Office.

USDA Forest Service, Gifford Pinchot National Forest. 1999. Gifford Pinchot National Forest Boundary, Region 6, USFS. vector digital data

US Geological Survey. USGS 14123500 Whit Salmon River near Underwood, WA. 2017. https://waterdata.usgs.gov/wa/nwis/inventory/?site_no=14123500USDA Natural Resources Conservation Service. SNOTEL Site Surprise Lakes. 2017. https://wcc.sc.egov.usda.gov/nwcc/site?sitenum=804

USDA Natural Resources Conservation Service. SNOTEL Site Potato Hill. 2017. https://wcc.sc.egov.usda.gov/nwcc/site?sitenum=702

Van Genuchten MT. A closed-form equation for predicting the hydraulic conductivity of unsaturated soils. Soil science society of America journal. 1980;44(5):892-8.

Van Mantgem PJ, Stephenson NL, Byrne JC, Daniels LD, Franklin JF, Fulé PZ, Harmon ME, Larson AJ, Smith JM, Taylor AH, Veblen TT. Widespread increase of tree mortality rates in the western United States. Science. 2009 Jan 23;323(5913):521-4.

Vehniäinen et al. 2016. Retene causes multifunctional transcriptomic changes in the heart of rainbow trout (Oncorhynchus mykiss) embryos. Environmental toxicology and pharmacology. 41:95-102.

Waring RH, Coops NC. Predicting large wildfires across western North America by modeling seasonal variation in soil water balance. Climatic change. 2016 Mar 1;135(2):325-39.

Webster R, Oliver MA. Geostatistics for environmental scientists. John Wiley & Sons; 2007 Oct 22.

Westerling AL, Hidalgo HG, Cayan DR, Swetnam TW. Warming and earlier spring increase western US forest wildfire activity. science. 2006 Aug 18;313(5789):940-3.

Wilcox BP, Wood MK, Tromble JM. Factors influencing infiltrability of semiarid mountain slopes. Journal of Range Management. 1988 May 1:197-206.

Wittenberg LE, Inbar M. The Role of Fire Disturbance on Runoff and Erosion Processes–a Long-Term Approach, Mt. Carmel Case Study, Israel. Geographical Research. 2009 Mar 1;47(1):46-56.

Zhu Q, Lin H, Doolittle J. Repeated electromagnetic induction surveys for determining subsurface hydrologic dynamics in an agricultural landscape. Soil Science Society of America Journal. 2010 Sep 1;74(5):1750-62.

Appendix

**A. Supplemental Figures:**

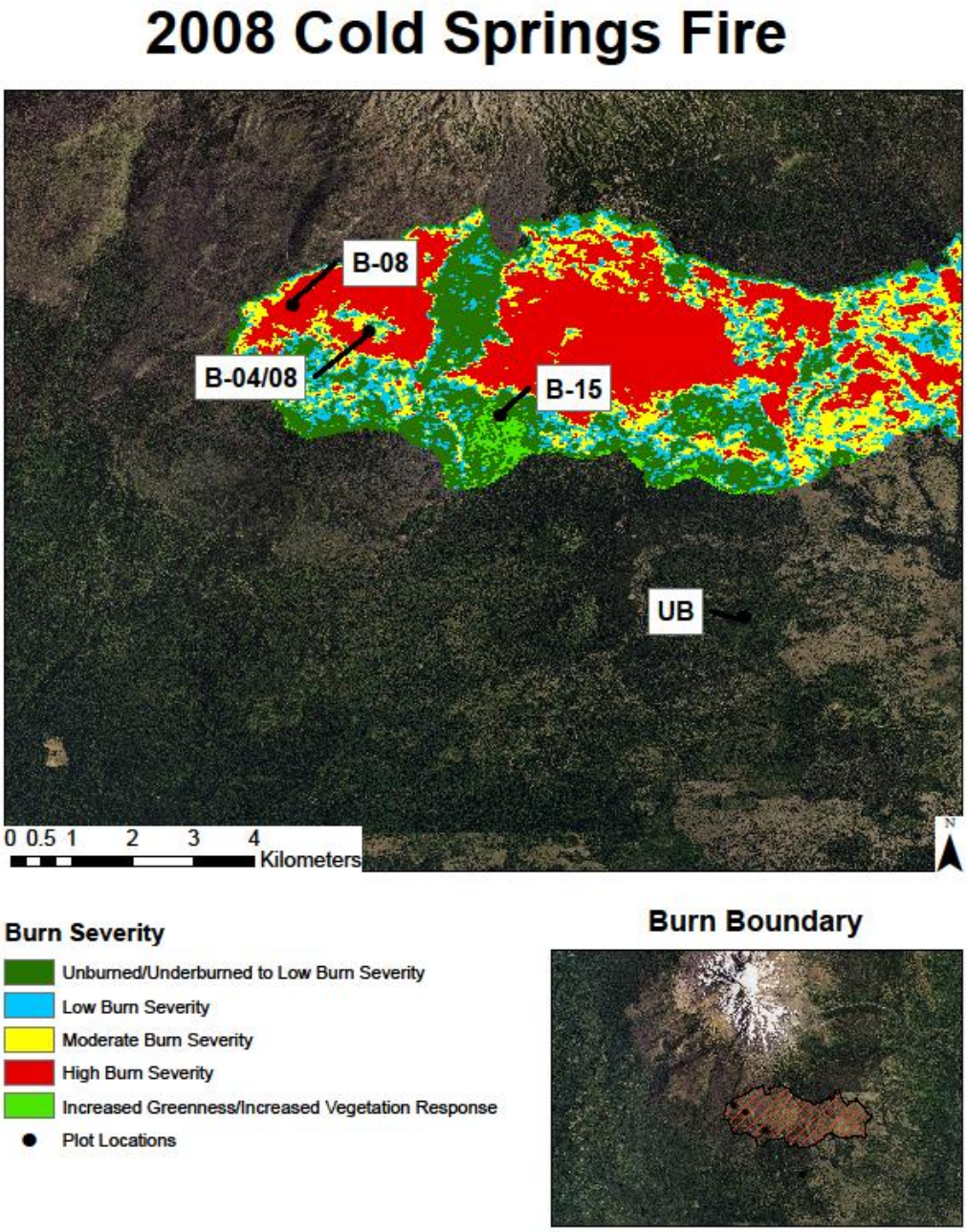


Supplemental Figure 1. 2008 Cold Springs Burn Severity. B-15 lies within the burn perimeter but was largely unaffected by the fire, as suggested by the severity map.

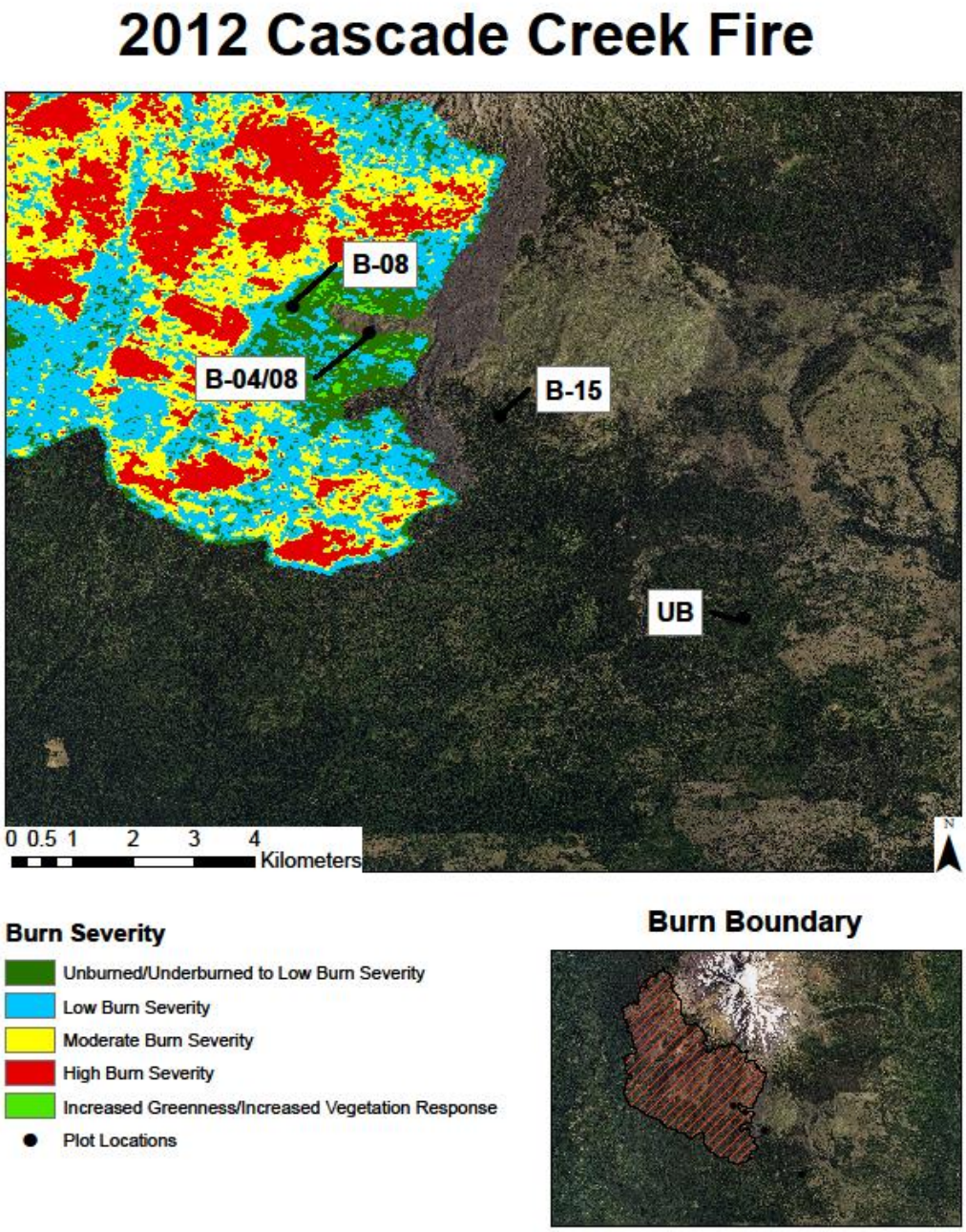


Supplemental Figure 2. 2012 Cascade Creek burn severity. All sites were unaffected by the fire.

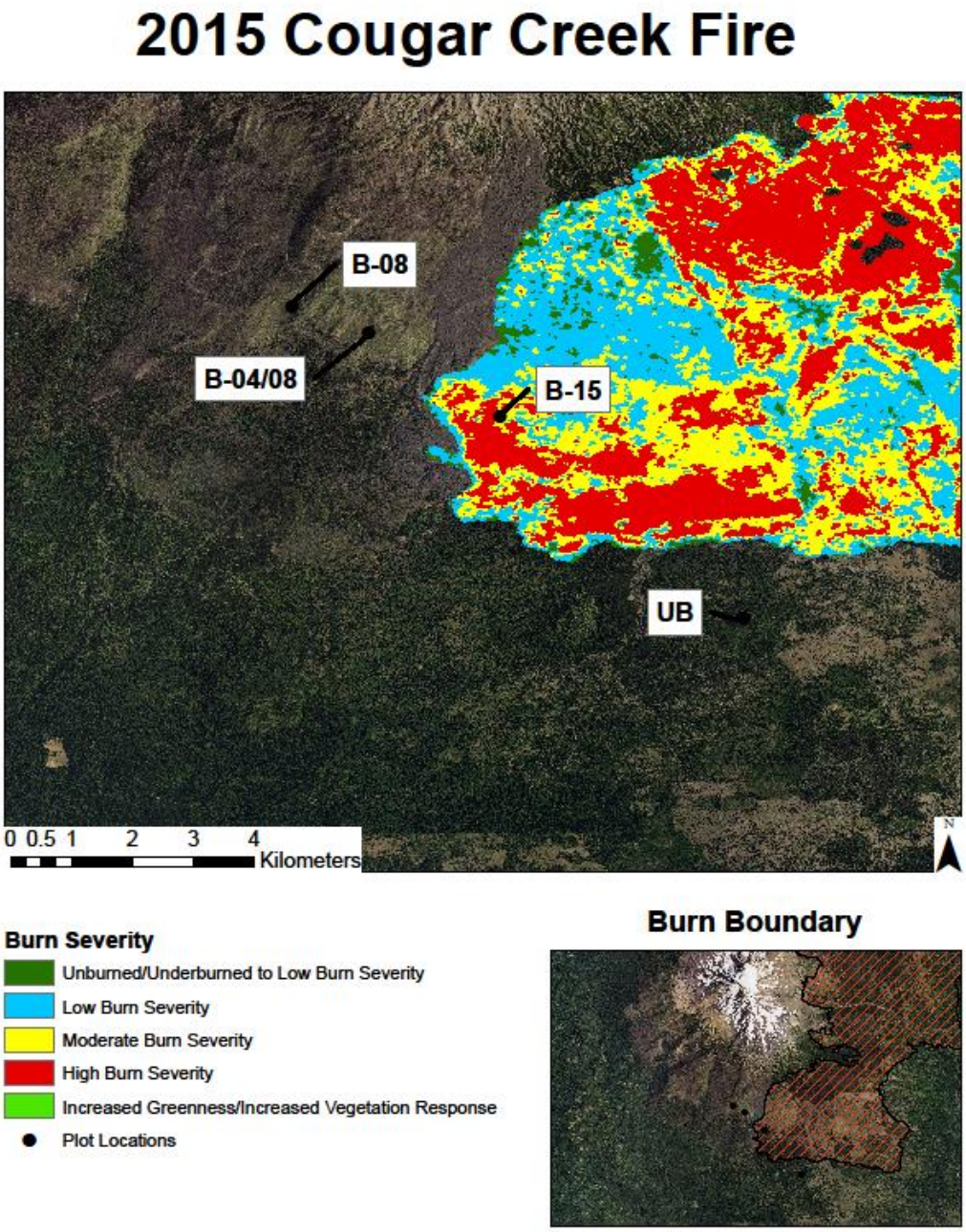


Supplemental Figure 3. 2015 Cougar Creek burn severity. B-15 is the only site affected by the Cougar Creek Fire.

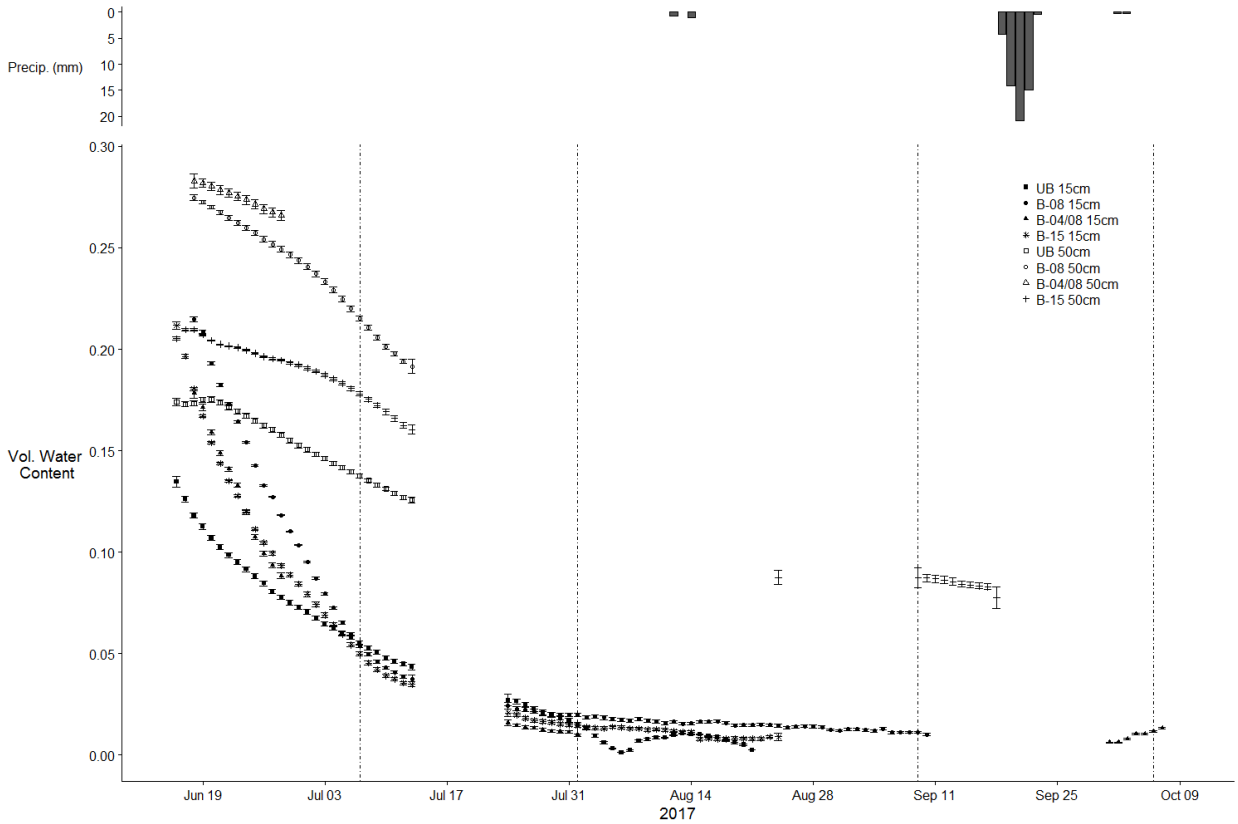


Supplemental Figure 4. Daily soil moisture drydown during the summer dry season. Precipitation was almost entirely absent during the season (top). For field measurements of volumetric water content (θ) over time, solid symbols represent probes placed at a depth of 15cm and hollow symbols represent probes placed at 50cm. Each point is a daily average of four probes recording at 30 min intervals (N=192 per point). Bars are the standard error. Vertical dashed lines are the dates of field surveying and geophysical EMI data collection.

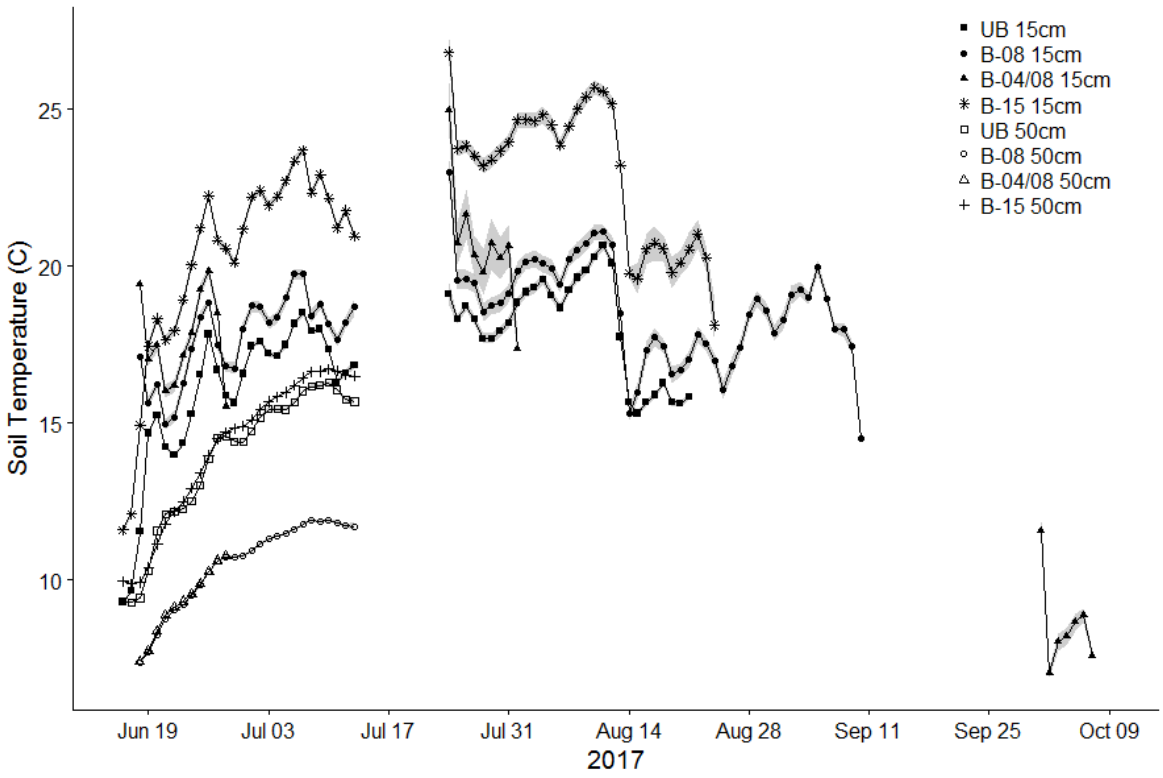


Supplemental Figure 5. Daily average soil temperature. Points are average soil temperatures for the respective plots and depths. Ribbon is the standard error of the mean.

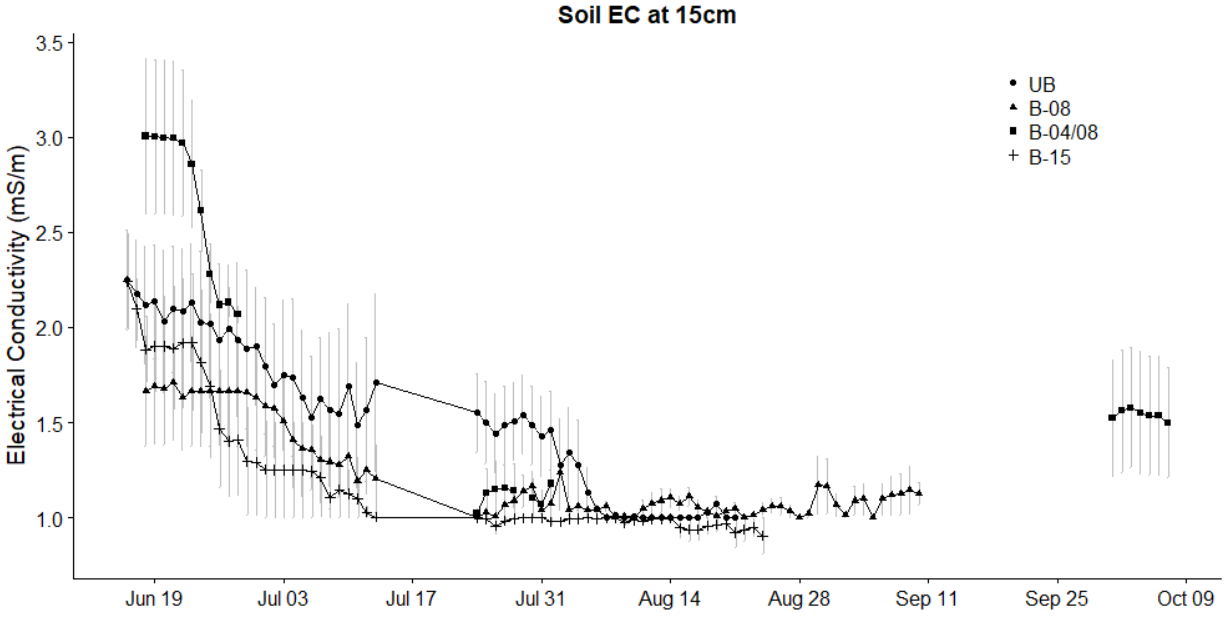


Supplemental Figure 6. Soil electrical conductivity at 15cm depth. Points are daily averages measured using Hydraprobes. Bars are the standard deviation.

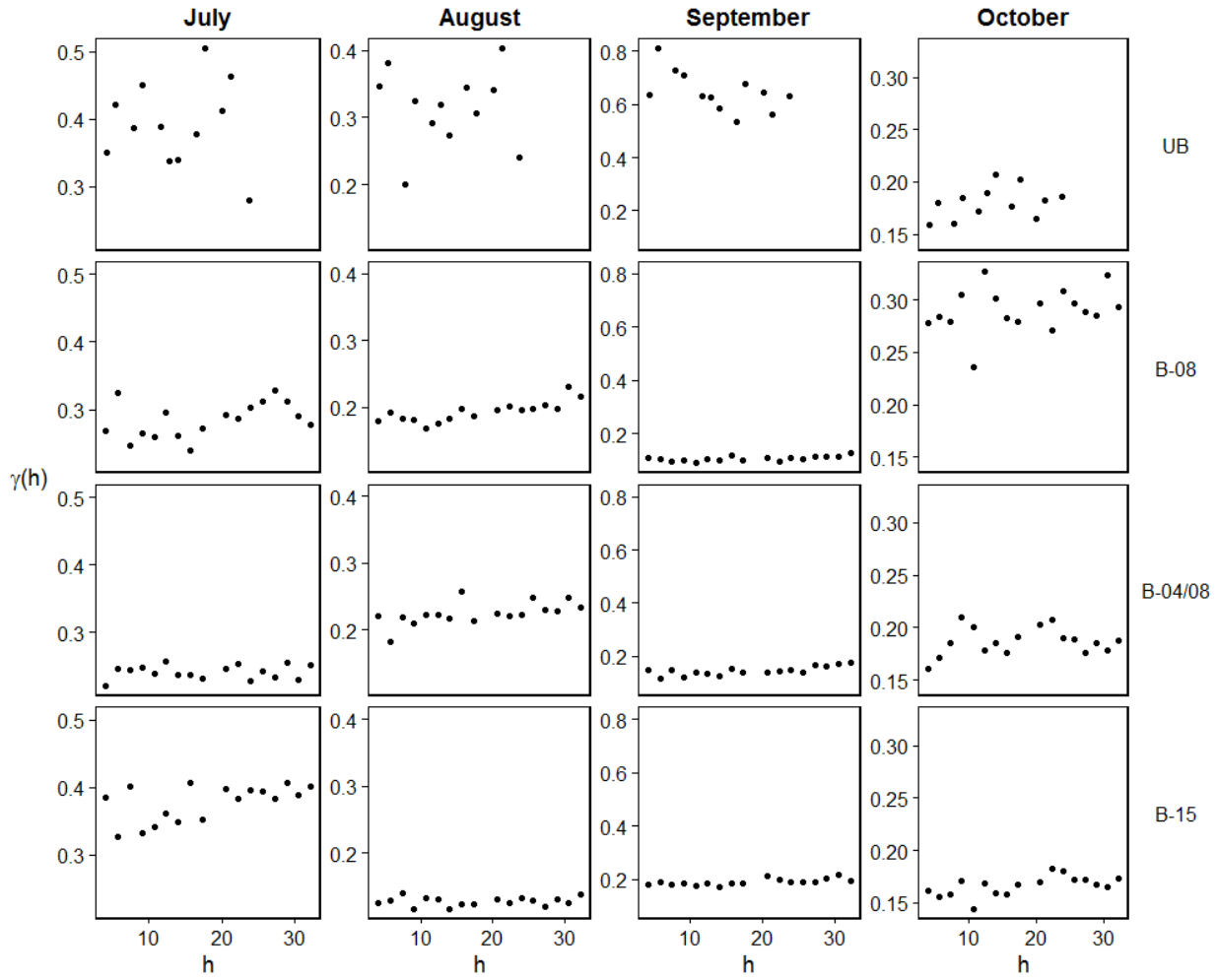


Supplemental Figure 7. Semi-variograms for each plot in each month for the 0-30cm layer. γ(h) is the semi-variance and h is the lag distance.

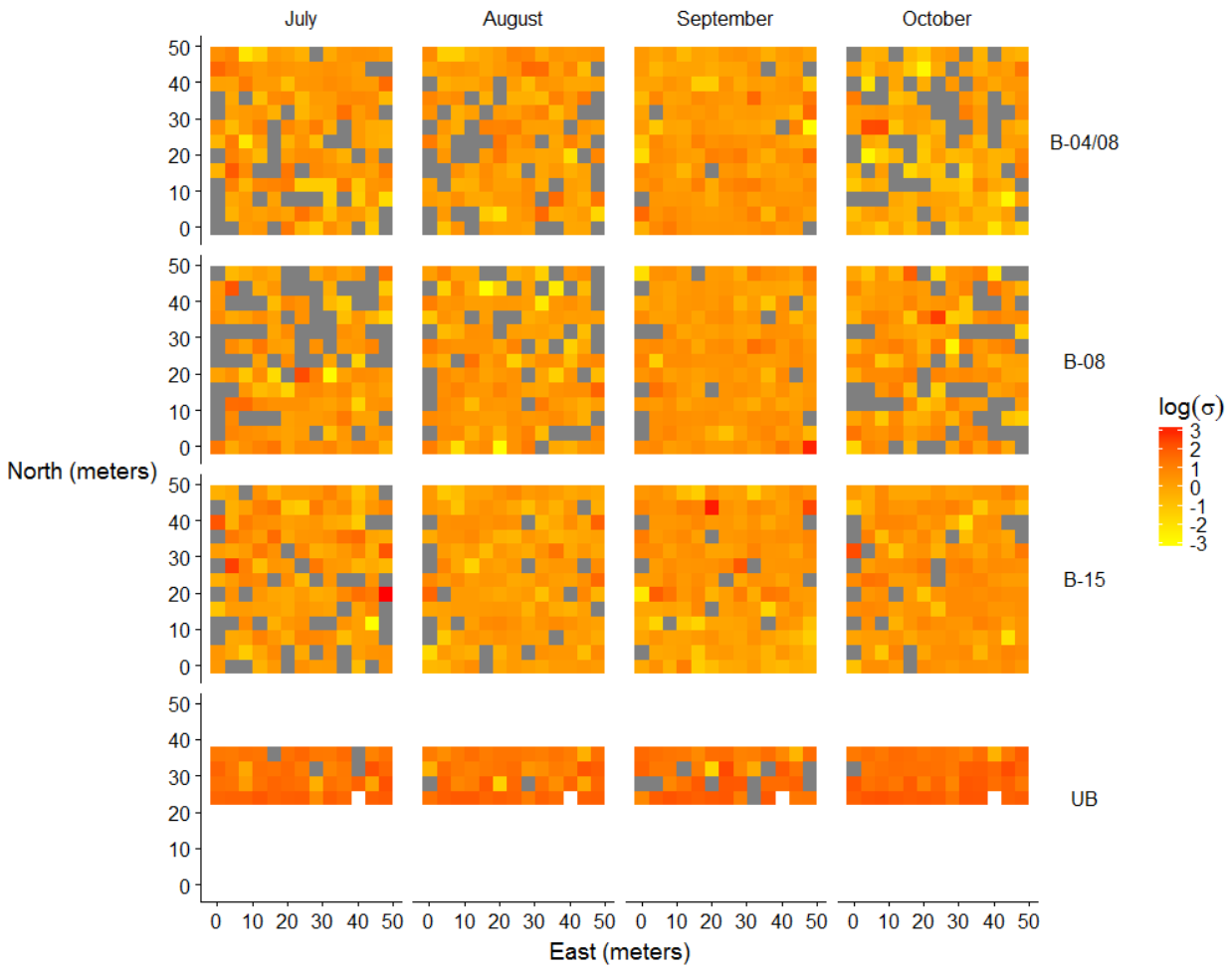


Supplemental Figure 8. Spatial variation of log-transformed ECa.

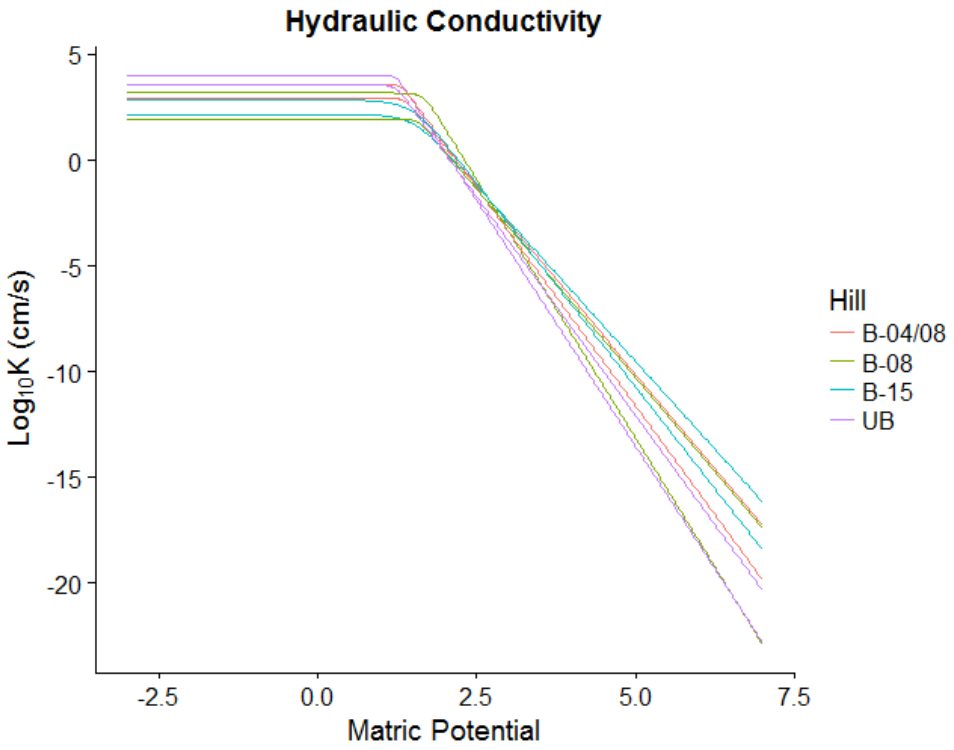


Supplemental Figure 9. Mualem Hydraulic Conductivity curves for each research plot. X-axis is the matric potential (kPa) in log scale.

## B. Supplemental Tables:

Supplemental Table 1. Species inventory and occurrence. Species present in a given plot are marked with an X.

| Forb/Herb | UB | B-15 | B-04/08 | B-08 |
|---|---|---|---|---|
| *Achillea millefolium* | | X | X | X |
| *Achyls triphylla* | X | | | |
| *Adenocaulon bicolor* | X | | | |
| *Agastache occidentalis* | | X | | X |
| *Aquilegia formosa* | | | | X |
| *Borago L.* | | X | | |
| *Chaenorhinum minus* | | X | | |
| *Chamerion angustifolium* | | | | X |
| *Claytonia parviflora* | | X | | |
| *Cochleariopsis groenlandica* | | X | | |
| *Cryptantha torreyana* | | X | | |
| *Epilobium brachycarpum* | | X | | X |
| *Epilobium minutum* | | X | X | X |
| *Galium triflorum* | X | | | |
| *Hieracium albiflorum* | X | X | | X |
| *Ipomoea L.* | | | | |
| *Lathyrus lanszwertii* | | X | | X |
| *Lomatium macrocarpum* | | X | | |
| *Lupinus lepidus* | | | X | |
| *Maianthemum stellatum* | X | | | |
| *Osmorhiza chilensis* | X | | | |
| *Penstemon euglaucus* | X | | X | |
| *Phacelia heterophylla* | | X | X | X |
| *Physalis grisea* | | | X | |
| *Polygonum aviculare* | | X | | |
| *Pteridium aquilinum* | X | | | |
| *Rumex acetosa* | | X | | |
| *Stellaria borealis* | X | X | | X |
| *Vicia americana* | | X | | X |
| *Viola bakeri* | | X | | |
| *Xerophyllum tenax* | | | X | X |

| Graminoid | UB | B-15 | B-04/08 | B-08 |
|---|---|---|---|---|
| *Achnatherum occidentale* | | X | X | |
| *Bromus carinatus* | X | | | |
| *Bromus inermis* | | X | | |
| *Bromus vulgaris* | | | | X |
| *Carex rossii* | | X | X | X |
| *Elymus elymoides* | | X | | |
| *Elymus glaucus* | | X | X | X |
| **Shrub** | | | | |
| *Arctostaphylos uva-ursi* | | | X | X |
| *Ceanothus velutinus* | | | | X |
| *Chimaphila umbellata* | X | | | |
| *Nothochelone nemorosa* | X | | | |
| *Prunus emarginata* | | X | X | X |
| *Ribes viscidulum* | | | | X |
| *Sambucus racemosa* | | | X | |
| *Spiraea densiflora* | X | | | |
| **Tree** | | | | |
| *Abies grandes* | X | | | |
| *Acer glabrum* | X | | | |
| *Pinus contorta* | | | | X |
| *Tsuga heterophylla* | | X | | |